platelets circulate in blood and secrete FVIII upon platelet activation in the vicinity of bleeding, so that local FVIII concentrations may be higher than that in the circulation.

We demonstrated efficient transduction of CB-CD34$^+$ cells by a SIV vector carrying the human FVIII gene. Taking advantage of their self-renewal and multi-lineage differentiation capabilities, transplantation of *ex vivo* engineered CB-CD34$^+$ cells enabled their engraftment in NOD/SCID mice, transgene expression, and human FVIII production. Because of xenograft transplantation, we transplanted human CD34$^+$ cells to NOD/SCID mice with myeloablation by irradiation. However, this gene therapy strategy can be potentially applicable to clinical studies because autologous transplantation of genetically transduced hematopoietic stem cells can be achieved with non-myeloablative conditioning [33]. Transplantation of *ex vivo* SIV vector-transduced CD34$^+$ cells without exposure of subjects to viral vectors is a useful approach with potential clinical application for gene therapy of hemophilia patients.

Gene therapy of human ADA-SCID and X-SCID by autologous transplantation of genetically modified hematopoietic stem cells has been shown to be very effective [33,34]. However, a leukemia-like disorder emerged in two X-SCID patients who received retrovirally mediated common $\gamma(\gamma c)$ gene transfer to hematopoietic stem cells [35]. This disorder appeared to be caused by insertion of the vector-derived γc gene in the LMO2 gene [35]. Similar to retrovirus vector-mediated gene transfer, random integration of the transgene to hematopoietic stem cell genomes takes place upon transduction by lentiviral vectors. Thus, vector-derived DNA insertion to such a leukemia-linked gene LMO2 can also happen in SIV vector-mediated FVIII gene transfer to hematopoietic stem cells. The SIV vector used in this study is designed to be a self-inactivating type vector to minimize activation of genes in the vicinity of the integration site. Thus FVIII gene transfer to hematopoietic stem cells by SIVhFVIII may be much safer than retrovirally mediated γc gene transfer to hematopoietic stem cells for X-SCID gene therapy. However, the risk of the inactivation of tumor suppressor genes still remains. Therefore, attempts such as the use of a regulated and cell-specific promoter, reduction of multiple insertion of the transgene into a single cell, and incorporation of a suicide gene into the vector should be studied to reduce the risk of development of an unpredictable disorder in the future.

Acknowledgements

We thank Dr. J. A. van Mourik for the full-length FVIII cDNA, Dr. Koichiro Tsuji, the Institute of Medical Science, the University of Tokyo, and Dr. Mika Wada, the Department of Pediatrics, Nihon University of Medicine, for advice on transplantation of human CB-CD34$^+$ cells into NOD/SCID mice. We also thank Ms. Fumino Muroi and Ms. Kou Kosaka for technical assistance with the human FVIII ELISA assay and purification of CB-CD34$^+$ cells. This work is supported in part by Health and Labour Sciences Research Grants from the Ministry of Health, Labour and Welfare and Grants-in-aid for Scientific Research from the Ministry of Education and Science. This manuscript was edited by IdEst, Inc.

References

1. Hoyer LW. Hemophilia A. *N Engl J Med* 1994; 330: 38–47.
2. Kay MA, High K. Gene therapy for the hemophilias. *Proc Natl Acad Sci U S A* 1999; 96: 9973–9975.
3. Kume A, Hanazono Y, Mizukami H, Urabe M, Ozawa K. Hematopoietic stem cell gene therapy: a current overview. *Int J Hematol* 1999; 68: 227–233.
4. Miyoshi H, Smith KA, Mosier DE, Verma IM, Torbett BE. Transduction of human CD34+ cells that mediate long-term engraftment of NOD/SCID mice by HIV vector. *Science* 1999; 283: 682–686.
5. Woods NB, Fahlman C, Mikkola H, *et al.* Lentiviral gene transfer into primary and secondary NOD/SCID repopulating cells. *Blood* 2000; 96: 3725–3733.
6. Scherr M, Battmer K, Blomer U, *et al.* Lentiviral gene transfer into peripheral blood-derived CD34$^+$ NOD/SCID-repopulating cells. *Blood* 2002; 99: 709–712.
7. Naldini L, Blomer U, Gallay P, *et al.* In vivo gene delivery and stable transduction of nondividing cells by a lentiviral vector. *Science* 1996; 272: 263–267.
8. Honjo S, Narita T, Kobayashi R, *et al.* Experimental infection of African green monkeys and cynomolgus monkeys with a SIVAGM strain isolated from a healthy African green monkey. *J Med Primatol* 1990; 19: 9–20.
9. Nakajima T, Nakamaru K, Ido E, Terao K, Hayami M, Hasegawa M. Development of novel simian immunodeficiency virus vectors carrying a dual gene expression system. *Hum Gene Ther* 2000; 11: 1863–1874.
10. Hoeben RC, Einerhand MP, Briet E, van Ormondt H, Valerio D, van der Eb AJ. Toward gene therapy in haemophilia A: retrovirus-mediated transfer of a factor VIII gene into murine haematopoietic progenitor cells. *Thromb Haemost* 1992; 67: 341–345.
11. Tonn T, Herder C, Becker S, Seifried E, Grez M. Generation and characterization of human hematopoietic cell lines expressing factor VIII. *J Hematother Stem Cell Res* 2002; 11: 695–704.
12. Kootstra NA, Matsumura R, Verma IM. Efficient production of human FVIII in hemophilic mice using lentiviral vectors. *Mol Ther* 2003; 7: 623–631.
13. Tiede A, Eder M, von Depka M, *et al.* Recombinant factor VIII expression in hematopoietic cells following lentiviral transduction. *Gene Ther* 2003; 10: 1917–1925.
14. Ogata K, Mimuro J, Kikuchi J, *et al.* Expression of human coagulation factor VIII in adipocytes transduced with the simian immunodeficiency virus agmTYO1-based vector for haemophilia A gene therapy. *Gene Ther* 2004; 11: 253–259.
15. Furukawa Y, Kikuchi J, Nakamura M, Iwase S, Yamada H, Matsuda M. Lineage-specific regulation of cell cycle control gene expression during haematopoietic cell differentiation. *Br J Haematol* 2000; 110: 663–673.
16. Ueda T, Tsuji K, Yoshino H, *et al.* Expansion of human NOD/SCID-repopulating cells by stem cell factor, Flk2/Flt3 ligand, thrombopoietin, IL-6, and soluble IL-6 receptor. *J Clin Invest* 2000; 105: 1013–1021.
17. Yoshino H, Ueda T, Kawahata M, *et al.* Natural killer cell depletion by anti-asialo GM1 antiserum treatment enhances human hematopoietic stem cell engraftment in NOD/Shi-scid mice. *Bone Marrow Transplant* 2000; 26: 1211–1216.
18. Ma F, Wada M, Yoshino H, *et al.* Development of human lymphohematopoietic stem and progenitor cells defined by expression of CD34 and CD81. *Blood* 2001; 97: 3755–3762.
19. Yonemura H, Sugawara K, Nakashima K, Nakahara Y, Hamamoto T, Mimaki I. Production of recombinant human factor VIII by co-expression of the heavy and light chains. *Protein Eng* 1993; 6: 669–674.
20. Chomczynski P, Sacchi N. Single-step method of RNA isolation by acid guanidinium thiocyanate-phenol-chloroform extraction. *Anal Biochem* 1987; 162: 156–159.
21. Sutton RE, Reitsma MJ, Uchida N, Brown PO. Transduction of human progenitor hematopoietic stem cells by human immunodeficiency virus type 1-based vectors is cell cycle dependent. *J Virol* 1999; 73: 3649–3660.

22. Xu R, Reems JA. Umbilical cord blood progeny cells that retain a CD34+ phenotype after ex vivo expansion have less engraftment potential than unexpanded CD34+ cells. *Transfusion* 2001; **41**: 213–218.
23. VandenDriessche T, Vanslembrouck V, Goovaerts I, *et al.* Long-term expression of human coagulation factor VIII and correction of hemophilia A after in vivo retroviral gene transfer in factor VIII-deficient mice. *Proc Natl Acad Sci U S A* 1999; **96**: 10379–10384.
24. Hoeben RC, Fallaux FJ, Van Tilburg NH, *et al.* Toward gene therapy for hemophilia A: long-term persistence of factor VIII-secreting fibroblasts after transplantation into immunodeficient mice. *Hum Gene Ther* 1993; **4**: 179–186.
25. Dwarki VJ, Belloni P, Nijjar T, *et al.* Gene therapy for hemophilia A: production of therapeutic levels of human factor VIII in vivo in mice. *Proc Natl Acad Sci U S A* 1995; **92**: 1023–1027.
26. Chuah MK, Van Damme A, Zwinnen H, *et al.* Long-term persistence of human bone marrow stromal cells transduced with factor VIII-retroviral vectors and transient production of therapeutic levels of human factor VIII in nonmyeloablated immunodeficient mice. *Hum Gene Ther* 2000; **11**: 729–738.
27. Naldini L, Verma IM. Lentiviral vectors. *Adv Virus Res* 2000; **55**: 599–609.
28. Chao H, Walsh CE. Induction of tolerance to human factor VIII in mice. *Blood* 2001; **97**: 3311–3312.
29. Roth DA, Tawa NE Jr, Proper JA, *et al.* The factor VIII transkaryotic therapy study group. Nonviral transfer of the gene encoding coagulation factor VIII in patients with severe hemophilia A. *N Engl J Med* 2001; **344**: 1782–1784.
30. Powell J, Ragni MV, White GC, *et al.* Phase 1 trial of FVIII gene transfer for severe hemophilia A using a retroviral construct administered by peripheral intravenous infusion. *Blood* 2003; **102**: 2038–2045.
31. Zennou V, Petit C, Guetard D, Nerhbass U, Montagnier L, Charneau P. HIV-1 genome nuclear import is mediated by a central DNA flap. *Cell* 2000; **101**: 173–185.
32. Sirven A, Pflumio F, Zennou V, *et al.* The human immunodeficiency virus type-1 central DNA flap is a crucial determinant for lentiviral vector nuclear import and gene transduction of human hematopoietic stem cells. *Blood* 2000; **96**: 4103–4110.
33. Aiuti A, Slavin S, Aker M, *et al.* Correction of ADA-SCID by stem cell gene therapy combined with nonmyeloablative conditioning. *Science* 2002; **28**: 2410–2413.
34. Hacein-Bey-Abina S, Le Deist F, Carlier F, *et al.* Sustained correction of X-linked severe combined immunodeficiency by *ex vivo* gene therapy. *N Engl J Med* 2002; **346**: 1185–1193.
35. Hacein-Bey-Abina S, von Kalle C, Schmidt M, *et al.* A serious adverse event after successful gene therapy for X-linked severe combined immunodeficiency. *N Engl J Med* 2003; **348**: 255–256.

Leukemia & Lymphoma, November 2004 Vol. 45 (11), pp. 2349–2351

Taylor&Francis
healthsciences

Severe Hepatitis and Complete Molecular Response Caused by Imatinib Mesylate: Possible Association of Its Serum Concentration with Clinical Outcomes

SATORU KIKUCHI[a], KAZUO MUROI[a,b,*], SATOKO TAKAHASHI[a], CHIZURU KAWANO-YAMAMOTO[a,b], MASAAKI TAKATOKU[a], AKIRA MIYAZATO[a], TADASHI NAGAI[a], MASAKI MORI[a,b], NORIO KOMATSU[a] and KEIYA OZAWA[a,b]

[a]*Division of Hematology, Department of Medicine, Jichi Medical School, Minamikawachi, Japan;* [b]*Division of Cell Transplantation and Transfusion, Jichi Medical School, Minamikawachi, Japan*

(Received 10 June 2004)

A 40-year-old female with chronic myelogeneous leukemia (CML) in the chronic phase was treated with imatinib mesylate (STI571) because of interferon resistance. She achieved complete cytogenetic response but not complete molecular response 3 months after STI571 administration. Six months later, she developed severe liver damage without evidence of actively infectious hepatitis A, B, C, G, E, TT virus, Epstein-Barr virus or cytomegalovirus. A significant serum level of STI571 (107 ng/ml) was detected, although she had not taken the drug for 6 days. Liver biopsy demonstrated massive hepatic necrosis, consistent with drug-induced hepatitis. She achieved complete molecular response, although she did not take STI571 for 47 days after the development of hepatitis. These results suggest that both hepatitis and molecular response were associated with the serum STI571 concentration.

Keywords: STI571; Serum concentration; Hepatitis; Molecular response

INTRODUCTION

STI571, an inhibitor of BCR-ABL tyrosine kinase, shows clinical activity in the treatment of CML in the chronic phase and less activity in the treatment of CML in blastic transformation [1–4]. Although STI571 has been well tolerated in clinical trials, various non-hematological adverse effects such as nausea, fluid retention, edema, muscle cramps and rash, most of which are mild, have been reported [5]. Recently, it has been reported that 3 female patients with CML treated with STI571 developed severe hepatitis [6,7]. We report a CML patient demonstrating both severe hepatitis and complete molecular response caused by STI571.

CASE REPORT

A 40-year-old female was diagnosed as having Philadelphia chromosome (Ph1)-positive CML in the chronic phase in December 1995 and received interferon soon after the diagnosis. Four months after interferon therapy, major cytogenetic response (Ph1, 1/29 cells) was obtained. Complete or major cytogenetic response was maintained from April 1996 to October 2000 by interferon alone. In November 2002, Ph1 in the bone marrow increased to 23/24 cells, although the interferon dose was increased. Therefore, STI571 at a daily dose of 400 mg started on January 2, 2003. At this time, there were no biochemical abnormalities including those of liver enzymes detected. The clinical course was uneventful and she had no adverse effects except slight leukocytopenia and anemia. On March 26, 2003, she achieved complete cytogenetic response in the bone marrow again. Although BCR-ABL messages were still detected by RT–PCR assay, 400 mg of STI571 was continuously given. On May 21, slight increase in aspartate aminotransferase (AST, 96U/l; normal range, 11–30) and alanine aminotransferase (ALT, 152 U/l; normal range, 4–30) but not total bilirubin (0.86 mg/dl; normal range, 0.29–1.03) was noticed. From June 5 to 7, she took STI571 but immediately vomited it. Between June 8 to 10, she did not take STI571 because of nausea. On June 11, she was admitted because of nausea and general fatigue (Fig. 1).

*Corresponding author. Address: Division of Cell Transplantation and Transfusion, Jichi Medical School, Minamikawachi, Tochigi 329-0498, Japan. Tel.: 81-285-44-2111. Fax: 81-285-44-5087. E-mail: muroi-kz@jichi.ac.jp

ISSN 1042-8194 print/ISSN 1029-2403 online © 2004 Taylor & Francis Ltd
DOI: 10.1080/10428190412331272721

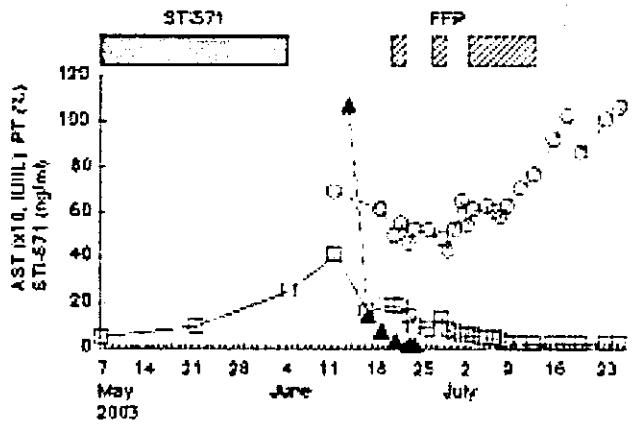

FIGURE 1 Clinical course. Open circles, open squares and filled triangles indicate percentage of prothrombin time, serum aspartate aminotransferase level and serum STI571 concentration, respectively. FFP, fresh frozen plasma.

Laboratory examination demonstrated increased levels of AST (406 U/l), ALT (559 U/l) and total bilirubin (2.7 mg/dl) and prolongation in prothrombin time (PT) (14.0 s, 69%; normal range, 10.4–12.2 s). The peripheral blood showed a hemoglobin level of 11.4 g/dl, a platelet count of 121 $\times$ 10^9/l, and a white blood cell count of 4.7 $\times$ 10^9/l with 57% neutrophils, 3% eosinophils, 1% basophils, 6% monocytes and 33% lymphocytes. Serological tests for IgM anti-hepatitis A virus (HAV) antibody, HBV surface antigen, HCV antibody and HEV antibody were negative. HGV, TT virus, HBV, HCV, cytomegalovirus and Epstein-Barr virus were not detected by the PCR method. Autoantibodies including antimitochondrial antibody and antismooth muscle antibody were negative. Ultrasonography of the abdomen showed nonspecific liver damage without gallstones. Computed tomography of the abdomen showed low-density lesions in the periportal areas of the liver, suggesting hepatitis.

She was suspected of having STI571-induced hepatitis [6], although drug lymphocyte-stimulating test for STI571 was negative. Residual STI571 in serum was demonstrated by liquid-chromatography tandem mass spectrometry [8] as follows: 107.0 ng/ml on June 13, 13.8 ng/ml on June 16, 7.4 ng/ml on June 18 and 3.6 ng/ml on June 20. STI571 had been discontinued since admission, however, total bilirubin increased to the maximum level of 9.98 mg/dl on June 27 and production of blood coagulation factors was impaired to 46% of PT, 39% of antithrombin III activity, 32% of protein C activity, and 139 mg/dl of fibrinogen on June 22. A total of 72 units of fresh frozen plasma were infused to replace coagulation factors produced in the liver. On July 23, percutaneous liver biopsy demonstrated severe centrolobular hepatic necrosis without evidence of veno-occlusive disease, consistent with drug-induced hepatitis [7]. Bone marrow aspiration the next day showed continuous complete cytogenetic response by conventional karyotypic analysis and there were no detectable BCR/ABL messages on RT–PCR. The patient was discharged on June 26 after recovery of hepatic function. On October 15, 2003, she still maintained normal blood counts with normal differential. A rechallenge test of STI571 has not been performed.

DISCUSSION

Our patient showed 2 important events during STI571 administration. One is drug-related liver toxicity. STI571 is not only metabolized by the cytochrome P450 enzymes, CYP3A4, CYP2C9 and CYP2D6 but also competitively inhibits CYP3A4 [9]. Drugs and foods inhibiting CYP3A4 such as erythromycin, clarithromycin, itraconazole and grapefruit juice increase the serum concentration of STI571 and lead to enhance STI571 toxicity in patients concurrently taking both STI571 and 1 of the CYP3A4-inhibiting agents [9]. Our patient took STI571 alone but not any agents, foods or supplements including herbs that affect CYP3A4. We do not know whether severe liver damage caused by STI571 is the result of immunologic idiosyncrasy (hypersensitivity reaction) or injury from a toxic metabolite (metabolic idiosyncrasy) [10]. Recently, Gambacorti-Passerini *et al.* have reported the pharmacokinetic analysis of STI571 in CML patients [11]. STI571 plasma concentrations were measured in 8 CML patients treated with 400 mg of the drug. After administration on day 1, peak concentration (C_{max}) of STI571 was achieved between 1 and 3 h; then in all of the patients, the drug was slowly cleared from plasma, being still detectable at 24 h. In 11 patients with CML treated with 400 mg, C_{max}, area under the curve in a 24-h period (24-h AUC) and half-life were 2.35 $\pm$ 1.0 μg/ml, 24.66 $\pm$ 8.5 μg.h/ml, and 12.5 $\pm$ 2.4 h, respectively. Similar analysis in healthy subjects treated with 400 mg of STI571 were shown in the CSTI571B2102 study conducted by Novartis Pharmaceuticals [12]: C_{max}, 1.56 $\pm$ 0.29 μg/ml; 24-h AUC, 16.30 $\pm$ 3.48 μg.h/ml; and half-life, 16.7 $\pm$ 3.1 h. Since a significant serum level of STI571 was detected 7 days after cessation of the drug administration in our patient, metabolic idiosyncrasy of STI571 in the liver is suggested. Interestingly, in our patient and others [6,7], severe liver damage caused by STI571 involved females in all cases. Therefore, we should carefully monitor STI571 administration to female patients with CML.

Another important finding in our patient is complete molecular response following severe liver damage caused by STI571. Before sustaining liver damage, the patient had achieved complete cytogenetic response but not complete molecular response by STI571. Complete molecular response was obtained followed by severe liver damage, although STI571 had not been given to the patient since the development of liver damage. As discussed above, severe liver damage in our patient was suggested to be associated with increased serum concentration of STI571. The achievement of complete molecular response may also have been caused by the

increased serum concentration of STI571. It is necessary to clarify the relationship between serum STI571 concentrations and clinical outcomes in CML patients.

Acknowledgments

The authors wish to thank doctors in the Division of Gastroenterology for useful suggestion on drug-induced hepatitis.

References

[1] Druker, B.J., Talpaz, M., Resta, D.J., Peng, B., Buchdunger, E., Ford, J.M., *et al.* (2001) "Efficacy and safety of a specific inhibitor of the BCR-ABL tyrosine kinase in chronic myeloid leukemia", *The New England Journal of Medicine*, **344**, 1031–1037.

[2] Sawyers, C.L., Hochhaus, A., Feldman, E., Goldman, J.M., Miller, C.B., Ottmann, O.G., *et al.* (2002) "Imatinib induces hematologic and cytogenetic responses in patients with chronic myelogenous leukemia in myeloid blast crisis: results of a phase II study", *Blood*, **99**, 3530–3539.

[3] Kantarjian, H., Sawyers, C., Hochhaus, A., Guilhot, F., Schiffer, C., Gambacorti-Passerini, C., *et al.* —International STI571 CML Study Group. (2002) "Hematologic and cytogenetic responses to imatinib mesylate in chronic myelogenous leukemia", *The New England Journal of Medicine*, **346**, 645–652.

[4] Kantarjian, H.M., Cortes, J., O'Brien, S., Giles, F.J., Albitar, M., Rios, M.B., *et al.* (2002) "Imatinib mesylate (STI571) therapy for Philadelphia chromosome-positive chronic myelogenous leukemia in blast phase", *Blood*, **99**, 3547–3553.

[5] Hensley, M.L. and Ford, J.M. (2003) "Imatinib treatment: Specific issues related to safety, fertility, and pregnancy", *Seminars in Hematology*, **40**(Suppl 3), 21–25.

[6] Ohyashiki, K., Kuriyama, Y., Nakajima, A., Tauchi, T., Ito, Y., Miyazawa, H., *et al.* (2002) "Imatinib mesylate-induced hepatotoxicity in chronic myeloid leukemia demonstrated focal necrosis resembling acute viral hepatitis", *Leukemia*, **16**, 2160–2161.

[7] James, C., Trouette, H., Marit, G., Cony-Makhoul, P. and Mahon, F.X. (2003) "Histological features of acute hepatitis after imatinib mesylate treatment", *Leukemia*, **7**, 978–979.

[8] Parise, R.A., Ramanathan, R.K., Hayes, M.J. and Egorin, M.J. (2003) "Liquid chromatographic-mass spectrometric assay for quantitation of imatinib and its main metabolite (CGP 74588) in plasma", *Journal of Chromatography. B. Analytical Technologies in the Biomedical and Life Sciences*, **791**, 39–44.

[9] O'Brien, S.G., Peng, B., Dutreix, C., Mehring, G., Milosavljev, S., Gapdeville, R., *et al.* (2001) "A pharmacokinetic interaction of glivec and simvastatin, a cytochrome 3A4 substrate, in patients with chronic myeloid leukemia", *Blood*, **98**, 141a (Abstract).

[10] Goodman, Z.D. (2002) "Drug hepatotoxicity", *Clinics in Liver Disease*, **6**, 381–397.

[11] Gambacorti-Passerini, C., Zucchetti, M., Russo, D., Frapolli, R., Verga, M., Bungaro, S., *et al.* (2003) "Alpha1 acid glycoprotein binds to imatinib (STI571) and substantially alters its pharmacokinetics in chronic myeloid leukemia patients", *Clinical Cancer Research*, **9**, 625–632.

[12] www.eudra.org/humandocs/PDFs/EPAR/glivec/24180len6.pdf

Topoisomerase inhibitors enhance the cytocidal effect of AAV-HSVtk/ganciclovir on head and neck cancer cells

TAKEHARU KANAZAWA[1,4], HIROAKI MIZUKAMI[1], HIROSHI NISHINO[2], TAKASHI OKADA[1], YUTAKA HANAZONO[1], AKIHIRO KUME[1], KEN KITAMURA[5], KEIICHI ICHIMURA[2] and KEIYA OZAWA[1,3]

[1]Division of Genetic Therapeutics, Center for Molecular Medicine, Departments of [2]Otolaryngology, and [3]Hematology, Jichi Medical School, 3311-1 Yakushiji Minamikawachi, Tochigi 329-0498; [4]Department of Otolaryngology, Faculty of Medicine, University of Ryukyus, 207 Uehara, Nishihara, Okinawa 903-0215; [5]Department of Otolaryngology, School of Medicine, Tokyo Medical and Dental University, 1-5-45 Yushima Bunkyo, Tokyo 113-8519, Japan

Received March 8, 2004; Accepted May 3, 2004

Abstract. Adeno-associated virus (AAV) is a non-pathogenic virus with a single-strand DNA genome. AAV vectors have several unique properties suited for gene therapy applications. However, an obstacle to their application is a low efficiency of transgene expression, mainly due to a limited second-strand synthesis. Previously, we reported that γ-rays enhanced the transduction efficiency and cytocidal effect of AAV vector harboring the herpes simplex virus-thymidine kinase (AAVtk) and ganciclovir (GCV) system. In the present study, we investigated whether topoisomerase inhibitors (etoposide and camptothecin) enhance the AAV vector-mediated transgene expression and the killing effect by AAVtk/GCV system. The enhancement of transgene expression was observed in a concentration-dependent manner on human laryngeal carcinoma cells (HEp-2 cells) and HeLa cells. Southern analysis confirmed that etoposide enhanced the double-strand synthesis of the AAV vector genome in HEp-2 cells and HeLa cells. The cells were efficiently killed by AAVtk/GCV system, as expected. More importantly, both etoposide and camptothecin augmented the cytocidal effect of the AAVtk/GCV system. These findings suggest that the combination of AAV-mediated suicide gene therapy and treatment with topoisomerase inhibitors may have synergistic therapeutic effects in the treatment of cancers.

Introduction

Advanced head and neck cancers exhibit a high mortality rate despite aggressive treatments involving surgery, radiotherapy, and chemotherapy. Patients often present with locally advanced conditions and the long-term survival rates have not improved appreciably over the past several decades. Current treatments for the advanced stages have shown little success, because tumors cannot be eradicated with an acceptable toxicity. One alternative strategy that has shown promise in the treatment of cancer is a gene therapy. Several virus vectors have been explored for the experiments of head and neck cancers, including retroviral (1), adenoviral (2) and adeno-associated virus (AAV) vectors (3). AAV is a non-pathogenic virus with a single-strand DNA genome (4,5). AAV vectors have emerged as a useful alternative to other vectors (6), and AAV have been evaluated in preclinical and clinical models for cystic fibrosis (7), Parkinson's disease (8) and hemophilia B (9). AAV vectors have a broad host range and can transduce head and neck cancer cells (3). However, an obstacle to their application is a low transgene expression efficiency, mainly due to limited second-strand synthesis (10,11). Genotoxic stresses such as chemotherapeutic agents, UV, heat shock, γ-ray irradiation have been reported to enhance the second-strand synthesis of the AAV vector genome and improve the transgene expression (12-15). Thus, an AAV vector encoding a suicide gene would kill target cells more efficiently when combined with other therapeutic agents. One well-studied suicide gene is the herpes simplex virus type-1 thymidine kinase (HSVtk)/ganciclovir (GCV) (16,17). Although the HSVtk/GCV enzyme/prodrug system has been shown to be effective for controlling tumor growth in animal models, it is difficult to eradicate cancer cells by the HSVtk/GCV system alone and tumors may recur after termination of the prodrug therapy (18-21). Thus, other therapeutic modalities, such as combination therapies, are under development (22,23). In our previous study, we demonstrated that γ-ray irradiation enhance AAV-mediated transgene expression and augmented the antitumor activity of HSVtk/GCV system on human head and neck cancer xenografts (24). Although radiotherapy has been one of the most valuable treatments for advanced head and neck cancer, chemotherapy with topoisomerase inhibitors has also been utilized. In this study, we explored the possibility of combining suicide gene therapy using the AAV vector with topoisomerase inhibitors, frequently used as chemotherapeutic agents, to enhance cytotoxicity, thereby providing a more effective means to control tumor growth.

Correspondence to: Dr Keiya Ozawa, Division of Genetic Therapeutics, Center for Molecular Medicine, Jichi Medical School, 3311-1 Yakushiji Minamikawachi, Tochigi 329-0498, Japan
E-mail: kozawa@ms.jichi.ac.jp

Key words: adeno-associated virus vector, herpes simplex thymidine kinase, head and neck neoplasms, topoisomerase inhibitor

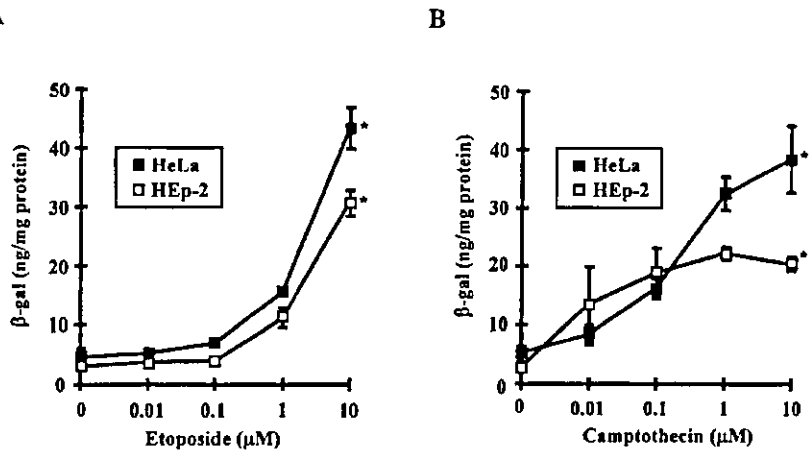

Figure 1. Effect of topoisomerase inhibitors on AAV vector-mediated transgene expression. HeLa cells (closed square) or HEp-2 cells (open square) were transduced with $1x10^3$ particles/cell of AAVLacZ 12-h pre-treatment with topoisomerase inhibitors. (A), The cells were pre-treated with etoposide at concentrations ranging from 0 to 10 μM. (B), The cells were pre-treated with camptothecin at concentrations ranging from 0 to 10 μM. Thirty-six hours after transduction, the expression levels of LacZ were assayed by using the ß-gal ELISA kit. Data were statistically analyzed by one-way ANOVA (*P<0.01).

Materials and methods

Cell lines. HeLa cells, 293 cells and the human laryngeal carcinoma HEp-2 cell line (a gift from the Cell Resource Center for Biomedical Research, Tohoku University), were cultured in DMEM/F12 (Gibco BRL, Grand Island, NY) supplemented with 10% heat-inactivated fetal bovine serum, 100 U/ml of penicillin and 100 μg/ml of streptomycin (Irvine Scientific, Santa Ana, CA) at 37°C in 5% CO_2.

Plasmids. The plasmid pAAVLacZ contains the CMV promoter, human growth hormone first intron, *Escherichia coli* LacZ gene, and SV40 early polyadenylation sequence between two inverted terminal repeats. A 1.8-kb DNA fragment encoding the HSVtk gene was obtained by double digestion with *Hin*cII and *Pvu*II of plasmid M2 (25) (a gift from Dr Y. Mishina, Yokohama City University, Japan) and subcloned into the pAAVLacZ in place of the LacZ gene (pAAVtk). pH19 is an AAV helper plasmid harbouring rep/cap sequences, and an adenovirus helper plasmid plAd5 contains the adenovirus early genes; E2a, E4, and VA.

AAV vector production. AAV vectors were produced based on the plasmid transfection (26). Briefly, subconfluent 293 cells were cotransfected with AAV vector plasmid, pH19, and plAd5 by a calcium phosphate-precipitation method. The cells were harvested and the recombinant AAV particles were released by three cycles of freeze/thaw. The vector solution was then purified through CsCl gradient twice as described previously (3). The vector titer was determined by a quantitative dot blot hybridization of DNase-treated stocks.

Transduction efficiency of HeLa or HEp-2 cells with AAV vectors. One day before transduction, $1x10^5$ cells were plated onto 3.5-cm dishes in triplicate. The cells were transduced with different amounts of AAVLacZ. Thirty-six hours after transduction with AAVLacZ, the amount of ß-galactosidase was quantitated by using the ß-gal ELISA kit (Boehringer-Mannheim, Hilden, Germany).

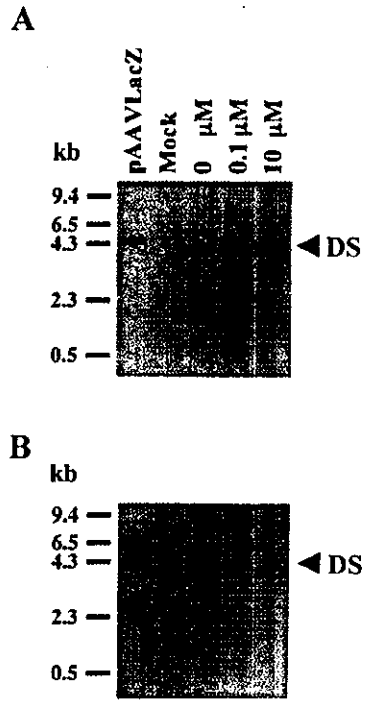

Figure 2. Second-strand synthesis of AAVLacZ genome after etoposide treatment in HeLa cells or HEp-2 cells. HeLa cells (A) or HEp-2 cells (B) were transduced with $1x10^4$ particles/cell of AAVLacZ following pre-treatment with 0, 0.1, 10 μM of etoposide. Two days later, total DNA was isolated. After mung bean nuclease treatment, the DNA samples were loaded on 1% agarose gels, transferred onto nylon membranes, and then hybridized with a radiolabeled CMV-specific probe. Signals were detected by using an imaging analyzer. Lane 1, a 4.7-kb fragment derived from pAAVLacZ; lane 2, mock-transduced; lanes 3-5, AAVLacZ-transduced following pre-treatment with etoposide (0, 0.1, 10 μM) treatment.

The enhancement of transgene expression by topoisomerase inhibitor treatment. The topoisomerase inhibitors used in this study were etoposide (Wako Pure Chemical, Osaka, Japan) and camptothecin (TopoGEN, Inc., Columbus, USA). Stock solutions of etoposide (10 mM) and camptothecin (10 mM)

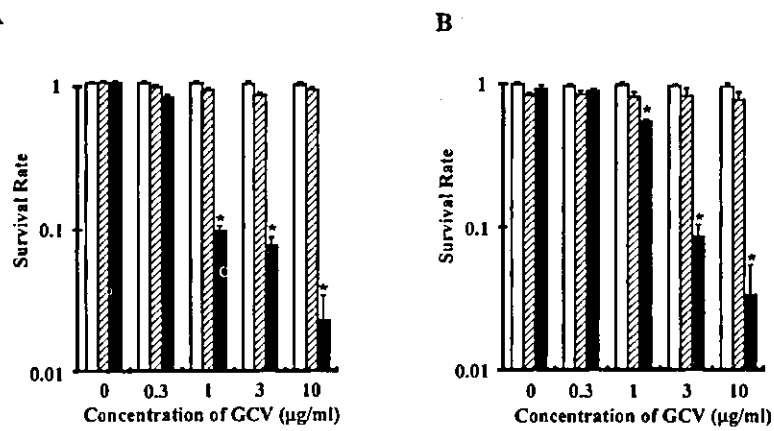

Figure 3. Survival of HeLa cells and HEp-2 cells upon AAVtk/GCV in terms of GCV concentration. HeLa cells (A) or HEp-2 cells (B) were mock-transduced (open bar), transduced with $3x10^5$ particles/cell of AAVLacZ (hatched bar), or AAVtk (closed bar). Twenty-four hours after transduction, the cells were exposed to different concentrations of GCV. Data were analyzed by two-way ANOVA. Asterisks mean that the data obtained for AAVtk-transduction were significantly different from those with or without transduction of AAVLacZ ($P<0.01$).

in dimethyl sulfoxide were stored at -20°C and diluted into PBS for use in experiments. HeLa cells and HEp-2 cells were treated with topoisomerase inhibitors for 12 h, washed twice with PBS, and then transduced with $1x10^3$ particles/cell of AAVLacZ. Thirty-six hours after transduction, we measured the amount of ß-galactosidase with the ß-gal ELISA kit (Boehringer-Mannheim).

Analysis of the second-strand synthesis of the vector genome. HeLa cells and HEp-2 cells grown in 10-cm dishes ($1x10^6$/dish) were transduced with $1x10^4$ particles/cell of AAVLacZ following pre-treatment with etoposide. Two days later, total DNA was isolated with the DNA Extractor WB kit (Wako Pure Chemical). Genomic DNA (40 μg) digested with 80 units of mung bean nuclease (Takara, Tokyo, Japan) were resolved on 1% agarose gels, transferred to nylon membranes (Hybond N^+; Amersham, Buckinghamshire, UK) in 50% formamide, 6X SSC, 0.5% sodium dodecyl sulfate, 5X Denhart's solution, and 100 μg/ml of denatured salmon sperm DNA at 42°C overnight. The membranes were washed, and then analyzed by using an image analyzer (BAS-1500, Fuji, Tokyo, Japan).

GCV treatment. The cells were plated and transduced with AAVtk at the dose of $1x10^5$ particles/cell. Twenty-four hours after transduction with AAV vectors, culture media were replaced by fresh media containing various concentrations of GCV ranging from 0 to 10 μg/ml. After a 7-day incubation in the presence of GCV, surviving cells were counted. The survival rate was calculated from the ratio of the number of cells not treated with GCV. To evaluate the synergistic effect of the AAVtk/GCV system and topoisomerase inhibitor treatment, the cells were transduced with AAVtk following either etoposide (0.1 μM, 10 μM) or camptothecin (0.01 μM, 1 μM) treatment.

Results

Effect of topoisomerase inhibitor on AAV-mediated transgene expression. The transduction efficiency of HEp-2 cells was almost as high as that of HeLa cells. The amount of ß-gal in HeLa cells were 220 μg/mg proteins, when the cells were transduced with $1x10^4$ particles/cell of AAVLacZ (24). Both etoposide and camptothecin have shown to increase the transduction efficiency with AAV vectors, mainly by accelerating the rate of leading strand synthesis of the AAV vector genome. In Fig. 1, etoposide and camptothecin treatment significantly increased LacZ expression in HeLa cells and HEp-2 cells in a concentration-dependent manner (one-way ANOVA: $P<0.01$).

Topoisomerase inhibitors enhance the second-strand synthesis of the AAV genome in HeLa and HEp-2 cells. To examine whether the second-strand synthesis of the AAV vector genome occurs more efficiently in the topoisomerase inhibitors treated-cells, HeLa cells and HEp-2 cells were treated with 0, 0.1, or 10 μM of etoposide, and then transduced with $1x10^4$ particles/cell of AAVLacZ. Forty-eight hours after transduction, total DNA was isolated, treated with mung bean nuclease, and then loaded on 1% agarose gels. After transfer to nylon membranes, signals corresponding to the AAVLacZ genomes were detected (Fig. 2). Mung bean nuclease was used to digest the single-strand DNA and to clearly visualize the double-stranded replicative form (DS) of the AAV vector genome. The DS was almost equal to 4.7-kb fragment derived from pAAVLacZ in size. At the concentration of 10 μM, in both HeLa and HEp-2 cells, the intensity of signal corresponding to the DS increased significantly, suggesting that the augmented transgene expression was associated with the conversion of the AAV vector genome to the double-stranded form.

The killing of HeLa and HEp-2 cells in terms of GCV concentration. Fig. 3 shows the killing effect of various concentration of GCV on HeLa cells (Fig. 3A) and HEp-2 cells (Fig. 3B) transduced with $3x10^5$ particles/cell of AAVtk (closed bar). When the AAVtk-transduced-cells were treated with 1 μg/ml of GCV, 90% of HeLa cells and 47% of HEp-2 cells were killed. As the concentration of GCV was increased, surviving cells were reduced and 98% of HeLa cells and 96% of HEp-2 cells were killed by the exposure to 10 μg/ml of GCV. This killing rate was significantly higher than that in

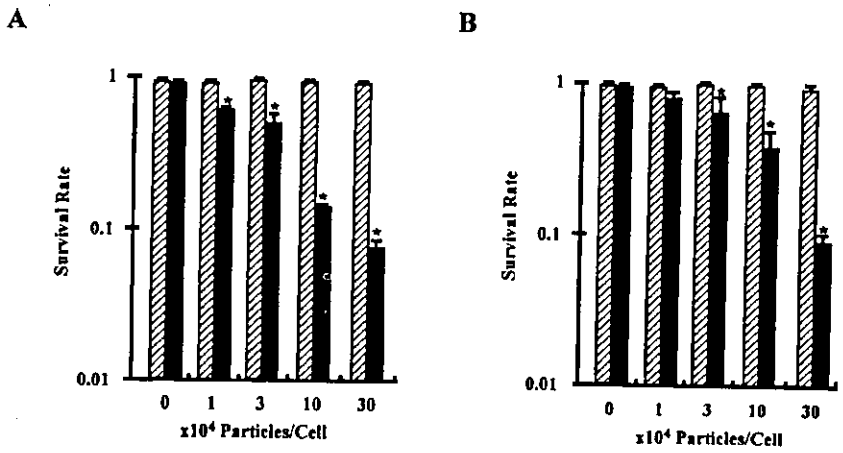

Figure 4. Survival of HeLa cells and HEp-2 cells upon AAVtk/GCV in terms of AAV doses. HeLa cells (A) or HEp-2 cells (B) were, transduced with various doses of AAVLacZ (hatched bar), or AAVtk (closed bar). Twenty-four hours after transduction, the cells were exposed to 3 μg/ml of GCV. Data were analyzed by two-way ANOVA. Asterisks mean that the data obtained for AAVtk-transduction were significantly different from those with or without transduction of AAVLacZ (P<0.01).

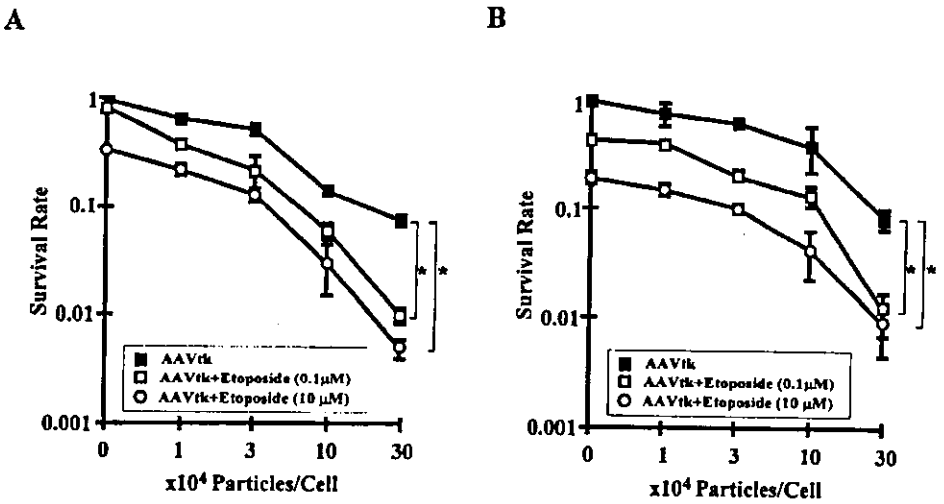

Figure 5. Enhancement of the cytocidal effect of AAVtk by etoposide. HeLa (A) or HEp-2 cells (B) were transduced with various concentrations of AAVtk with or without etoposide treatment. Twenty-four hours after transduction, the cells were treated with 3 μg/ml of GCV. Closed squares: AAVtk-transduced cells. Open squares: AAVtk-transduced with etoposide treatment (0.1 μM). Open circles: AAVtk-transduced cells with etoposide treatment (10 μM). Asterisks mean that the AAVtk-transduced and etoposide treated cells were significantly different from the AAVtk-transduced and non-treated cells (P<0.01).

AAVLacZ-transduced cells (hatched bar) or mock-transduced cells (open bar) (two-way ANOVA: P<0.01).

The killing of HeLa and HEp-2 cells in terms of AAV vector dose. Fig. 4 shows the killing effect of GCV (3 μg/ml) on HeLa cells and HEp-2 cells transduced with various doses of AAVtk. When HeLa cells were transduced with $3x10^4$ particles/cell of AAVtk, 50% of the cells were killed upon exposure to GCV. As the dose of AAVtk was increased, the number of surviving cells was reduced. This killing rate was significantly higher than that in the case of AAVLacZ-transduced cells, as expected (Fig. 4A). Similarly, AAVtk-transduced HEp-2 cells were killed by exposure to GCV, which was significantly higher than the killing rate in AAVLacZ-transduced cells (Fig. 4B) (two-way ANOVA: P<0.01).

Enhanced cytocidal effect of the AAVtk/GCV system by topoisomerase inhibitors (etoposide or camptothecin). To investigate whether etoposide treatment enhances the killing effect of AAVtk/GCV, HeLa (Fig. 5A) and HEp-2 cells (Fig. 5B) were transduced with various doses of AAVtk following pre-treatment with 0.1 μM or 10 μM etoposide, and then cultured in GCV (3 μg/ml). When HeLa cells were transduced with $3x10^4$ particles/cell of AAVtk, 53% of the 0.1 μM treated cells and 84% of the 10 μM treated cells were killed by the addition of GCV. When HeLa cells were transduced at $3x10^5$ particles/

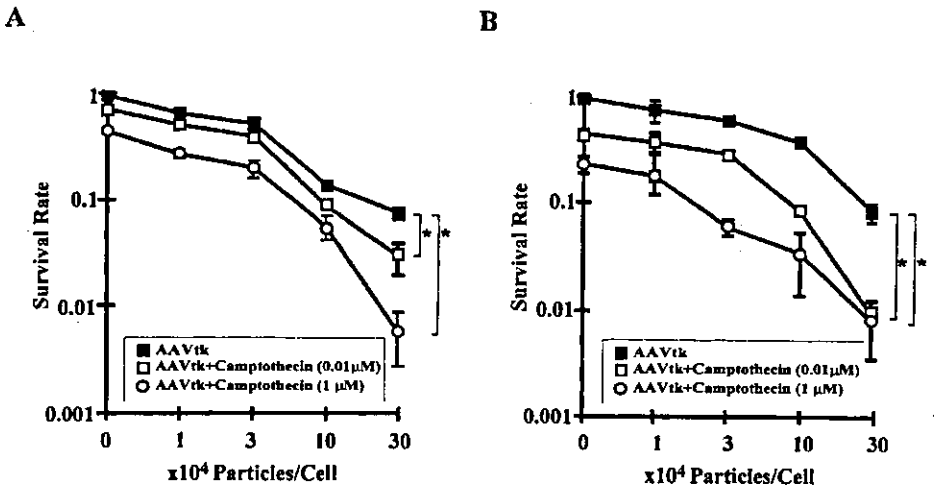

Figure 6. Enhancement of the cytocidal effect of AAVtk by camptothecin. HeLa (A) or HEp-2 cells (B) were transduced with various doses of AAVtk with or without camptothecin treatment. Twenty-four hours after transduction, the cells were treated with 3 μg/ml of GCV. Closed squares: AAVtk-transduced cells. Open squares: AAVtk-transduced with camptothecin treatment (0.01 μM). Open circles: AAVtk-transduced cells with camptothecin treatment (1 μM). Asterisks mean that the AAVtk-transduced and camptothecin treated cells were significantly different from the AAVtk-transduced and non-treated cells ($P<0.01$).

cell, etoposide enhanced the killing effects of AAVtk/GCV system by 21-fold. Etoposide treatment also enhanced the killing effects on HEp-2 cells by 5-fold. The enhancement by etoposide treatment was calculated from the ratio of 10 μM-treated survival rate to non-treated survival rate. These results show that etoposide treatment enhances the killing effects of AAVtk/GCV system significantly (two-way ANOVA: $P<0.01$). Similarly, we examined whether camptothecin treatment enhanced the killing effect of AAVtk/GCV. When HeLa cells were transduced at $3x10^5$ particles/cell, the combined therapy with camptothecin and AAVtk/GCV killed 12-fold HeLa cells (Fig. 6A) and 9-fold HEp-2 cells (Fig. 6B), compared with AAVtk/GCV system alone. These results show that camptothecin treatment also enhances the killing effects of AAVtk/GCV system significantly (two-way ANOVA: $P<0.01$).

Discussion

The application of AAV vectors to gene therapy for head and neck cancer is limited by their low transduction efficiency. Our previous studies showed the enhancement of AAV vector-mediated transgene expression and killing effect of AAVtk/GCV on the head and neck cancer cells by γ-ray (3). In this study, we demonstrated that topoisomerase inhibitors enhanced AAV vector-mediated transgene expression and cytocidal effect of AAVtk/GCV on target cells. The enhanced transgene expression and killing effect can be explained by the higher conversion efficiency of AAV vector genome to double-stranded form. In fact, we demonstrated that topoisomerase inhibitors augmented the second-strand synthesis and transgene expression on the cancer cells. Topoisomerase inhibitors have been utilized as chemotherapeutic agents. Topoisomerases are known to catalyze the reversible breakage and rejoining of DNA to check the DNA unwind during replication (27). Although etoposide and camptothecin inhibit different enzymes, both can induce similar DNA repair function.

It is unclear what kind of host DNA polymerases require for the conversion of single-stranded vector genomes to double-stranded molecules. According to the study that compared the transduction efficiency of dividing cells to non-dividing cells (13), DNA repair synthesis or other activities associated with DNA repair require transduction rather than replicative DNA synthesis. Some unspecified DNA repair mechanism activated by topoisomerase inhibitors may contribute to enhance the second-strand synthesis of AAV vector genome.

Since the mechanism of enhancement of transgene expression has vital significance for the use of AAV vectors, several studies have focused on this topic. Qing *et al* (28) reported that dephosphorylation of the single-stranded D sequence-binding protein facilitated second-strand synthesis of the AAV vector genome. Sanlioglu *et al* (29) reported that the enhancement of AAV vector transduction by UV and adenovirus E4orf6 correlated with induction of two distinct molecular conversion pathways, and UV led to increased abundance of circular AAV vector genome. However, the precise mechanisms by which genotoxic agents facilitate second-strand synthesis of AAV vector genome remains unknown.

Several studies reported that AAV vectors were useful for the treatment of cancers in model experiments. Kunke *et al* (30) showed that expressing the antisense of human papillomavirus early gene effectively killed the tumors derived from cervical cancer cells. In suicide gene therapy, HSVtk-expressing AAV vectors have been reported in the application to several kinds of cancer. The AAV vectors expressing HSVtk and interleukin 2 effectively killed glioma cells implanted into brains of nude mice (31). The expression of HSVtk driven by a liver-specific promoter via AAV vectors in tumors experimentally produced by implantation of hepatocellular carcinoma cells successfully retarded the tumor progression (32). We previously demonstrated the enhancement of the cytocidal effect of AAVtk/GCV system by γ-ray *in vitro*

and *in vivo* (3,24). As shown in Fig. 4, the AAVtk/GCV system effectively killed the cancer cells depending on the concentration of GCV. Furthermore, when the cancer cells were treated with topoisomerase inhibitors prior to transduction, they were killed more efficiently in a concentration-dependent manner (Figs. 5 and 6).

The combination therapy using other vectors and chemotherapy have been reported (15,33), but the augmentation of the second-strand synthesis by chemotherapeutic agent is unique to AAV vectors. Favorably, apoptosis induced by topoisomerase treatment enhance the bystander effects, which may allow nearby untransduced cells to take up the apoptotic vesicles containing phosphorylated toxic GCV metabolites. Thus, the combination therapy of AAV-mediated suicide gene therapy with chemotherapeutic agents or other genotoxic stress such as radiotherapy seems to be valuable for the treatment of cancers.

Recently, the HSVtk mutants with improved GCV mediated killing and bystander effect have been developed (34,35). Since GCV has side effects such as pancytopenia and acute renal failure, the concentration of GCV should be kept as low as possible. Our model would be another alternative to improve AAV-mediated suicide gene therapy of cancer. Although several studies were reported on combining chemotherapy and viral vector-mediated gene therapy (15,33), our therapeutic model made it with acceptable concentrations of topoisomerase inhibitors. AAV-mediated suicide gene therapy and chemotherapy may provide a more effective and safer alternative for the treatment of head and neck cancer.

Acknowledgements

We thank Avigen Inc., for providing the plasmids, pAAVLacZ, pH19 and plAd5. We also thank the Cell Resource Center for Biomedical Research, Tohoku University for providing the HEp-2 cells. This work was supported in part by grants from the Ministry of Health, Labor and Welfare of Japan, Grants-in-Aid for Science Research from the Ministry of Education, Culture, Sports, Science and Technology of Japan, and Special Co-ordination Funds for promoting Science and Technology of the Science and Technology Agency of the Japanese Government.

References

1. Hamstra DA, Rice DJ, Fahmy S, Ross BD and Rehemtulla A: Enzyme/prodrug therapy for head and neck cancer using a catalytically superior cytosine deaminase. Hum Gene Ther 10: 1993-2003, 1999.
2. Clayman GL, El-Naggar AK, Roth JA, *et al*: *In vivo* molecular therapy with p53 adenovirus for microscopic residual head and neck squamous carcinoma. Cancer Res 55: 1-6, 1995.
3. Kanazawa T, Urabe M, Mizukami H, *et al*: Gamma-rays enhance rAAV-mediated transgene expression and cytocidal effect of AAV-HSVtk/ganciclovir on cancer cells. Cancer Gene Ther 8: 99-106, 2001.
4. Berns KI and Rose JA: Evidence for a single-stranded adenovirus-associated virus genome: isolation and separation of complementary single strands. J Virol 5: 693-699, 1970.
5. Blacklow NR, Hoggan MD, Sereno MS, *et al*: A seroepidemiologic study of adenovirus-associated virus infection in infants and children. Am J Epidemiol 94: 359-366, 1971.
6. Bueler H: Adeno-associated viral vectors for gene transfer and gene therapy. Biol Chem 380: 613-622, 1999.
7. Wagner JA, Reynolds T, Moran ML, *et al*: Efficient and persistent gene transfer of AAV-CFTR in maxillary sinus. Lancet 351: 1702-1703, 1998.
8. Muramatsu S, Fujimoto K, Ikeguchi K, *et al*: Behavioral recovery in a primate model of Parkinson's disease by triple transduction of striatal cells with adeno-associated viral vectors expressing dopamine-synthesizing enzymes. Hum Gene Ther 13: 345-354, 2002.
9. Kay MA, Manno CS, Ragni MV, *et al*: Evidence for gene transfer and expression of factor IX in haemophilia B patients treated with an AAV vector. Nat Genet 24: 257-261, 2000.
10. Ferrari FK, Samulski T, Shenk T and Samulski RJ: Second-strand synthesis is a rate-limiting step for efficient transduction by recombinant adeno-associated virus vectors. J Virol 70: 3227-3234, 1996.
11. Fisher KJ, Gao GP, Weitzman MD, De Matteo R, Burda JF and Wilson JM: Transduction with recombinant adeno-associated virus for gene therapy is limited by leading-strand synthesis. J Virol 70: 520-532, 1996.
12. Alexander IE, Russell DW and Miller AD: DNA-damaging agents greatly increase the transduction of non-dividing cells by adeno-associated virus vectors. J Virol 68: 8282-8287, 1994.
13. Russell DW, Alexander IE and Miller AD: DNA synthesis and topoisomerase inhibitors increase transduction by adeno-associated virus vectors. Proc Natl Acad Sci USA 92: 5719-5723, 1995.
14. Alexander IE, Russell DW, Spence AM and Miller AD: Effects of gamma irradiation on the transduction of dividing and non-dividing cells in brain and muscle of rats by adeno-associated virus vectors. Hum Gene Ther 7: 841-850, 1996.
15. Peng D, Qian C, Sun Y, Barajas MA and Prieto J: Transduction of hepatocellular carcinoma (HCC) using recombinant adeno-associated virus (rAAV): *in vitro* and *in vivo* effects of genotoxic agents. J Hepatol 32: 975-985, 2000.
16. Furman PA, McGuirt PV, Keller PM, Fyfe JA and Elion GB: Inhibition by acyclovir of cell growth and DNA synthesis of cells biochemically transformed with herpesvirus genetic information. Virology 102: 420-430, 1980.
17. Cheng YC, Grill SP, Dutschman GE, Nakayama K and Bastow KF: Metabolism of 9-(1,3-dihydroxy-2-propoxymethyl) guanine, a new anti-herpes virus compound, in herpes simplex virus-infected cells. J Biol Chem 258: 12460-12464, 1983.
18. Trask TW, Trask RP, Aguilar-Cordova E, *et al*: Phase I study of adenoviral delivery of the HSV-tk gene and ganciclovir administration in patients with current malignant brain tumors. Mol Ther 1: 195-203, 2000.
19. Hasenburg A, Tong XW, Rojas-Martinez A, *et al*: Thymidine kinase gene therapy with concomitant topotecan chemotherapy for recurrent ovarian cancer. Cancer Gene Ther 7: 839-844, 2000.
20. Sutton MA, Freund CT, Berkman SA, *et al*: *In vivo* adenovirus-mediated suicide gene therapy of orthotopic bladder cancer. Mol Ther 2: 211-217, 2000.
21. Makinen K, Loimas S, Wahlfors J, Alhava E and Janne J: Evaluation of herpes simplex thymidine kinase mediated gene therapy in experimental pancreatic cancer. J Gene Med 2: 361-367, 2000.
22. Kawashita Y, Ohtsuru A, Kaneda Y, *et al*: Regression of hepatocellular carcinoma *in vitro* and *in vivo* by radiosensitizing suicide gene therapy under the inducible and spatial control of radiation. Hum Gene Ther 10: 1509-1519, 1999.
23. Rogulski KR, Wing MS, Paielli DL, Gilbert JD, Kim JH and Freytag SO: Double suicide gene therapy augments the anti-tumor activity of a replication-competent lytic adenovirus through enhanced cytotoxicity and radiosensitization. Hum Gene Ther 11: 67-76, 2000.
24. Kanazawa T, Mizukami H, Okada T, *et al*: Suicide gene therapy using AAV-HSVtk/ganciclovir in combination with irradiation results in regression of human head and neck cancer xenografts in nude mice. Gene Ther 10: 51-58, 2003.
25. Wilkie NM, Clements JB, Boll W, Mantei N, Lonsdale D and Weissmann C: Hybrid plasmids containing an active thymidine kinase gene of Herpes simplex virus 1. Nucleic Acids Res 7: 859-877, 1979.
26. Matsushita T, Elliger S, Elliger C, *et al*: Adeno-associated virus vectors can be efficiently produced without helper virus. Gene Ther 5: 938-945, 1998.
27. Wang JC: DNA topoisomerases. Annu Rev Biochem 65: 635-692, 1996.

28. Qing K, Khuntirat B, Mah C, *et al*: Adeno-associated virus type 2-mediated gene transfer: correlation of tyrosine phosphorylation of the cellular single-stranded D sequence-binding protein with transgene expression in human cells *in vitro* and murine tissues *in vivo*. J Virol 72: 1593-1599, 1998.
29. Sanlioglu S, Duan D and Engelhardt JF: Two independent molecular pathways for recombinant adeno-associated virus genome conversion occur after UV-C and E4orf6 augmentation of transduction. Hum Gene Ther 10: 591-602, 1999.
30. Kunke D, Grimm D, Denger S, *et al*: Preclinical study on gene therapy of cervical carcinoma using adeno-associated virus vectors. Cancer Gene Ther 7: 766-777, 2000.
31. Okada H, Miyamura K, Itoh T, *et al*: Gene therapy against an experimental glioma using adeno-associated virus vectors. Gene Ther 3: 957-964, 1996.
32. Su H, Lu R, Chang JC and Kan YW: Tissue-specific expression of herpes simplex virus thymidine kinase gene delivered by adeno-associated virus inhibits the growth of human hepatocellular carcinoma in athymic mice. Proc Natl Acad Sci USA 94: 13891-13896, 1997.
33. Reid T, Galanis E, Abbruzzese J, *et al*: Intra-arterial administration of a replication-selective adenovirus (dl1520) in patients with colorectal carcinoma metastatic to the liver: a phase I trial. Gene Ther 8: 1618-1626, 2001.
34. Qiao J, Black ME and Caruso M: Enhanced ganciclovir killing and bystander effect of human tumor cells transduced with a retroviral vector carrying a herpes simplex virus thymidine kinase gene mutant. Hum Gene Ther 11: 1569-1576, 2000.
35. Valerie K, Brust D, Farnsworth J, *et al*: Improved radiosensitization of rat glioma cells with adenovirus-expressed mutant herpes simplex virus-thymidine kinase in combination with acyclovir. Cancer Gene Ther 7: 879-884, 2000.

Translocation and cleavage of myocardial dystrophin as a common pathway to advanced heart failure: A scheme for the progression of cardiac dysfunction

Teruhiko Toyo-Oka*†‡§, Tomie Kawada¶, Jumi Nakata*, Han Xie*, Masashi Urabe‖, Fujiko Masui*, Takashi Ebisawa*, Asaki Tezuka*, Kuniaki Iwasawa†‡, Toshiaki Nakajima‡, Yoshio Uehara†, Hiroyuki Kumagai**, Sawa Kostin††, Jutta Schaper††, Mikio Nakazawa‡‡, and Keiya Ozawa‖

*Department of Pathophysiology and Internal Medicine, †Health Service Center, and ‡Department of Cardiovascular Medicine, University of Tokyo, Tokyo 113-0033, Japan; ¶Division of Pharmacy and ‡‡Department of Medical Technology, Niigata University, Niigata 951-8520, Japan; ‖Division of Gene Therapy, Jichi Medical School, Tochigi 329-0498, Japan; **Department of Pharmacology, Gunma University, Maebashi 371-8511, Japan; and ††Department of Experimental Cardiology, Max Planck Institute, Bad Nauheim 61231, Germany

Communicated by Setsuro Ebashi, Okazaki National Research Institutes, Okazaki, Japan, March 25, 2004 (received for review January 24, 2004)

Advanced heart failure (HF) is the leading cause of death in developed countries. The mechanism underlying the progression of cardiac dysfunction needs to be clarified to establish approaches to prevention or treatment. Here, using TO-2 hamsters with hereditary dilated cardiomyopathy, we show age-dependent cleavage and translocation of myocardial dystrophin (Dys) from the sarcolemma (SL) to the myoplasm, increased SL permeability *in situ*, and a close relationship between the loss of Dys and hemodynamic indices. In addition, we observed a surprising correlation between the amount of Dys and the survival rate. Dys disruption is not an epiphenomenon but directly precedes progression to advanced HF, because long-lasting transfer of the missing *δ-SG* gene to degrading cardiomyocytes *in vivo* with biologically nontoxic recombinant adenoassociated virus (rAAV) vector ameliorated all of the pathological features and changed the disease prognosis. Furthermore, acute HF after isoproterenol toxicity and chronic HF after coronary ligation in rats both time-dependently cause Dys disruption in the degrading myocardium. Dys cleavage was also detected in human hearts from patients with dilated cardiomyopathy of unidentified etiology, supporting a scheme consisting of SL instability, Dys cleavage, and translocation of Dys from the SL to the myoplasm, irrespective of an acute or chronic disease course and a hereditary or acquired origin. Hereditary HF may be curable with gene therapy, once the responsible gene is identified and precisely corrected.

Despite the steady progress of pharmaceutical therapy, it is still difficult to completely prevent heart failure (HF) from proceeding to an advanced stage. Cardiac transplantation is the last choice to save the patient at the end stage, and this treatment entails many sociomedical problems. An alternative strategy for therapy is urgently required (1, 2). Primary or secondary degradation of dystrophin (Dys) might be of great significance in determining the cause of HF. Muscular dystrophy results in HF, and poor outcome in patients and animal models is associated with genetic mutations of Dys or the sarcoglycan (SG) complex (1–6). In the present study, we examined the following phenomena: (*i*) the time course of the hemodynamics with biventricular catheterization under stable anesthesia (7) until the TO-2 animals started to show overt HF and cardiac death; (*ii*) *in situ* sarcolemma (SL) stability by double fluoromicroscopy for the entry of an SL-impermeable dye, Evans blue dye (EB), into cardiomyocytes (8) and immunostaining of Dys or δ-SG; (*iii*) Western blotting of Dys and protein quantification; (*iv*) the correlation between limited proteolysis of Dys and hemodynamics; and (*v*) *in vivo* gene transduction in TO-2 hamsters. We also evaluated pathological features in rats with acute and acquired HF due to isoproterenol (Isp) toxicity (9) and in humans with advanced dilated cardiomyopathy (DCM).

Materials and Methods

Experimental Animals, the *rAAV* Vector Gene Construct, and *in Vivo* Gene Delivery. Male F_1B (control) and TO-2 hamster strains were obtained from Bio Breeders (Watertown, MA), and rAAV/lacZ vector alone or a mixture of recombinant adenoassociated virus (rAAV)/lacZ and rAAV/δ-SG was intramurally injected into the cardiac apex of the 5-week-old hamsters (7). pW1, an rAAV plasmid containing lacZ or a 1.2-kb fragment of δ-SG cDNA flanked by inverted terminal repeats of the AAV genome, pHLP19, a helper plasmid with *rep* and *cap* genes, and pladeno-1, a plasmid harboring the adenovirus *E2A*, *E4*, and *VA* genes, were used for rAAV/lacZ or rAAV/δ-SG production. pWSG with a δ-SG expression cassette driven by a cytomegalovirus (CMV) promoter was used for rAAV/δ-SG production (7, 8). Under open chest surgery with constant-volume ventilation, rAAV/lacZ alone or a mixture of rAAV/lacZ and rAAV/δ-SG was intramurally injected into the cardiac apex twice (each injection was 15 μl, for a total of 8.4×10^{10} and 6×10^{10} copies for lacZ and δ-SG, respectively).

Morphological and Immunological Analyses. A polyclonal, site-directed antibody to δ-SG was prepared at a high titer, by using a synthetic peptide with a sequence deduced from the cloned cDNA as a specific epitope (4). Monoclonal antibodies to Dys and to the transgene of lacZ (β-galactosidase) were obtained from NovoCastra (Newcastle, U.K.) and Funakoshi (Tokyo). The density of antibody-specific bands for the rod domain of Dys was measured within a linear intensity range for the applied amount of protein, after Western blotting of whole-heart homogenates, by 5–15% SDS/PAGE. For the Isp study, 10–20% SDS/PAGE was used to detect degradation products of both Dys and δ-SG. To simultaneously monitor Dys disruption, SL fragility *in situ*, and expression of the δ-SG transgene, double fluoromicroscopy was used to detect immunostaining of Dys with a FITC-labeled antibody specific to the rod domain of Dys, the entry of membrane-impermeable EB into cardiomyocytes, and immunostaining of δ-SG with a rhodium isothiocyanate (RITC)-labeled specific antibody by using a Nikon Diaphot or a Leica (Heidelberg, Germany) TCS SL confocal microscope. Where indicated, the Dys immunoproduct in the SL and myoplasm was semiquantified on cardiomyocytes, with or without transduction of δ-SG in the same observation field.

Abbreviations: HF, heart failure; Dys, dystrophin; SG, sarcoglycan; SL, sarcolemma; EB, Evans blue dye; Isp, isoproterenol; DCM, dilated cardiomyopathy; rAAV, recombinant adenoassociated virus; LVP, left ventricular pressure; EDP, end diastolic pressure; CVP, central venous pressure.

§To whom correspondence should be addressed. E-mail: toyooka_3im@hotmail.com.

Table 1. Cardiac hemodynamics with progression of HF

Strain	Age, weeks	LVP, mmHg	dP/dt_{max}, mmHg/sec	dP/dt_{min}, mmHg/sec	EDP, mmHg	CVP, mmHg
F_1B	5	82.9 ± 1.2	4,385 ± 91	−4,503 ± 208	3.1 ± 0.6	1.70 ± 0.53
	15	132.9 ± 5.5†	8,188 ± 743†	−7,188 ± 971†	1.8 ± 1.5	0.78 ± 0.50
	25	132.5 ± 6.9	6,709 ± 188	−6,513 ± 602	1.7 ± 2.7	0.46 ± 0.21
	40	125.1 ± 9.6	7,063 ± 290	−7,180 ± 576	1.6 ± 0.9	−0.62 ± 0.32
TO-2	5	83.0 ± 2.1	4,599 ± 192	−5,175 ± 233*	1.9 ± 0.3*	2.82 ± 0.17*
	15	100.2 ± 4.7*†	4,645 ± 637*	−3,664 ± 378*†	8.8 ± 1.9*†	2.70 ± 0.87*
	25	87.9 ± 8.3*	5,240 ± 388*	−3,171 ± 80*	12.8 ± 1.6*	3.12 ± 0.88*
	40	80.0 ± 2.8*	4,283 ± 97*	−3,120 ± 145*	18.0 ± 1.4*†	9.35 ± 1.35*†

Hemodynamic indices measured under stable anesthesia (7, 8): LVP, its maximum derivative (dP/dt_{max}) and minimum derivative (dP/dt_{min}), EDP, and CVP, in control (F_1B strain) and hereditary DCM (TO-2 strain) hamsters. Each value is shown as the mean ± SE (n = 4–8 hamsters in each group). * and † indicate statistical significance ($P < 0.05$) compared with the F_1B strain and the preceding age, respectively.

Hemodynamic Studies and Statistical Analyses. Peak left ventricular pressure (LVP), left ventricular end diastolic pressure (EDP), its first derivative (dP/dt), and central venous pressure (CVP) were measured under stable anesthesia (7, 8). All values were expressed as the mean ± SE and evaluated by paired Student's t test, ANOVA, and correlation analyses. A P value of <0.05 was considered significant.

Results and Discussion

Progression of DCM to Advanced HF in TO-2 Hamsters. Control F_1B hamsters showed growth-dependent increases in the peak LVP, the maximum rate of LVP (dP/dt_{max}), and the minimum rate of LVP (dP/dt_{min}, Table 1). In contrast, TO-2 hamsters persistently demonstrated systolic failure characterized by reduced LVP, dP/dt_{max}, and blunted dP/dt_{min}. Congestive HF was documented by increased left ventricular EDP and CVP. These signs became aggravated between 25 and 40 weeks of age, when the rate of cardiac death sharply increased (see below). The EDP and CVP reached levels 9.5 and 3.3 times higher, respectively, than those at 5 weeks of age.

Translocation of Dys from the SL to the Myoplasm During DCM Progression. Cardiac samples from TO-2 hamsters revealed time-dependent pathological features at each age (Fig. 1). After 5 weeks, double fluoromicroscopy showed that Dys was neatly arranged on the SL, and EB administered *i.v.* before killing the animals did not enter the myoplasm, indicating that the integrity of the SL was well preserved. After 25 and 40 weeks, the Dys on the SL became blurred, and some cardiomyocytes demonstrated a shift of Dys from the SL to the myoplasm. We refer to this phenomenon as "translocation" of Dys. These cardiomyocytes matched exactly with cells that took up EB (within ovals), denoting that the SL of the translocated cells leaked the exogenously applied dye.

Cleavage of Dys in Hamster Heart and in the Hearts of Humans with DCM. Western blotting of the myocardial homogenate with an antibody specific to the rod domain of Dys showed characteristic features (Fig. 2*a Left*). Normal hearts at 5 weeks of age showed a band at 430 kDa corresponding to normal Dys, and the staining intensity was preserved up to 40 weeks of age. Striking differences were observed in TO-2 hamsters, although at 5 and 15 weeks of age the staining pattern did not differ from that of the F_1B heart. However, at 25 weeks of age, extra bands were detected between 60 and 200 kDa (Fig. 2*a Left*), and the intensity of the Dys 430-kDa band started to decline. The intensity of this band was markedly reduced between 25 and 40 weeks of age, whereas the intensity of the 60-kDa band increased, mirroring the Dys band (Fig. 2*b*). The period of significant Dys cleavage matched exactly the periods when Dys translocation became

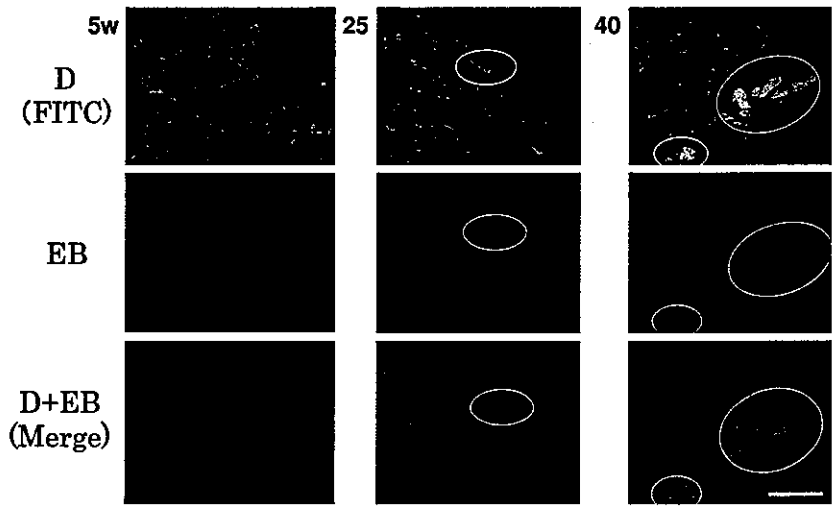

Fig. 1. Age-dependent translocation of Dys and increased permeability of the SL during HF progression in TO-2 hamsters. Double fluoromicroscopy for detection of a FITC-labeled antibody to the rod domain of Dys and entry of membrane-impermeable, fluorescent EB, at 5, 25, and 40 weeks of age (w). Cardiomyocytes demonstrating a shift of Dys from the SL to the myoplasm are shown in ovals. (Bar = 40 μm.)

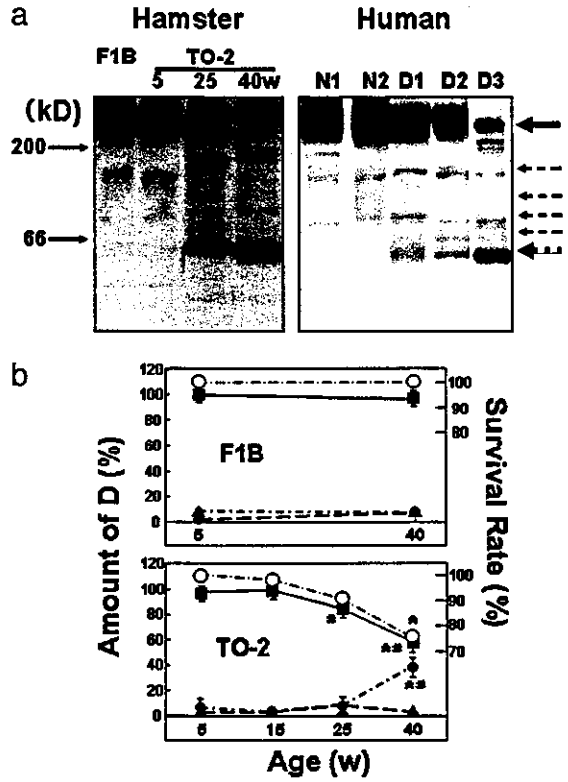

Fig. 2. Cleavage and reduction of cardiac Dys during DCM progression in hamsters and humans. (*a Left*) Control (F_1B strain) or DCM (TO-2 strain) hamsters at 5, 25, and 40 weeks of age (w). (*a Right*) Normal human myocardium (N1 and N2) and DCM hearts (D1, D2, and D3) at the time of cardiac transplantation. A solid arrow at 430 kDa and several dotted arrows denote the original Dys and its degradation products, respectively, after 5–20% SDS/PAGE of whole-heart homogenates. (*b*) Time course of the survival rate of control (F_1B; *Upper*) or DCM (TO-2; *Lower*) hamsters (○) and the density of immunoreactive bands specific to the rod domain of Dys at 430 (■), 60 (●) or 160 (▲) kDa. * and # indicate a significant difference, compared with the control F_1B strain and the preceding age, respectively.

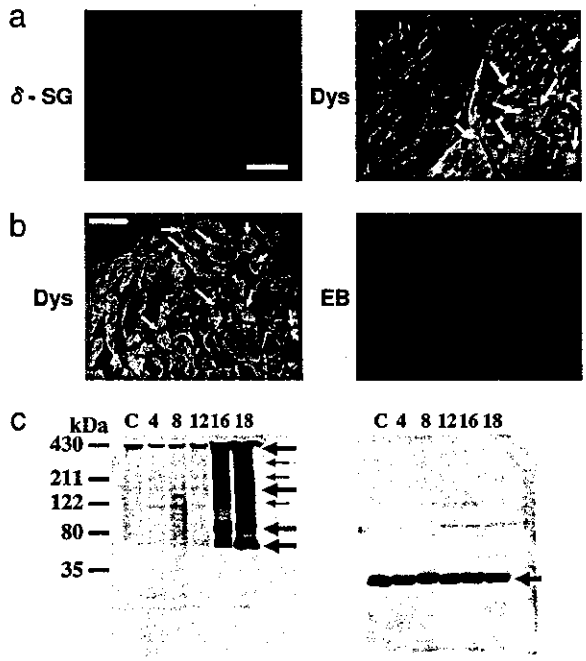

Fig. 3. (*a*) Double immunostaining of δ-SG (rhodamine isothiocyanate) and Dys (FITC) of TO-2 hamster hearts 35 weeks after local δ-SG gene transfection *in vivo* (8). Arrows indicate cardiomyocytes where dystrophin was translocated from the SL to the myoplasm. (Bar = 40 μm.) (*b*) Assessment of Dys translocation (FITC) and SL fragility *in situ* (EB entry) 16 h after the administration of Isp at a high dose (10 mg/kg i.p.) in Wistar rats (15). Arrows indicate cardiomyocytes where dystrophin was translocated from the SL to the myoplasm. (Bar = 40 μm.) (*c*) Western blotting of Dys (*Left*) and δ-SG (*Right*) from the same rat heart homogenate sample after gradient 10–15% SDS/PAGE of the control (C) and 4, 8, 12, 16 and 18 h after Isp treatment. Arrows indicate uncleaved Dys (430 kDa) and Dys degradation products (*Left*) or δ-SG (*Right*).

evident (Fig. 1) and when the animals started to die of congestive HF (ref. 8 and Fig. 2*b*). The intensity of the faint 160-kDa band did not change throughout the study and appeared to be unrelated to the progression of HF.

Similar cleavage of Dys was confirmed in hearts from patients with DCM of unidentified etiology who had undergone cardiac transplantation (Fig. 2*a Right*). The topological shift of Dys was also documented in samples of advanced stage DCM (unpublished data). Accordingly, the translocation was common to both animal models and patients with DCM. Other antibodies to the C or N terminus of Dys did not clearly recognize the cleavage product (data not shown). At present, we do not know the reason for this discrepancy in human cases of advanced HF showing selective cleavage of Dys at the N terminus (10).

Relationship of Dys Cleavage to Hemodynamics and the Lifespan of Hamsters. Surprisingly, the amount of Dys or its 60-kDa-band degradation product in TO-2 animals very closely correlated with the hemodynamic indices that characterize the progression of HF. The Dys amount was positively correlated with the systolic index [peak LVP, coefficient of regression (r) = 0.998 and $P < 0.0004$], and negatively correlated with the diastolic parameters (EDP, $r = 0.996$ and $P < 0.0005$; CVP, $r = 0.954$ and $P < 0.002$). The intensity of the 60-kDa band showed a clear negative correlation with the LVP ($r = 0.961$, $P < 0.002$) and a positive correlation with the EDP ($r = 0.954$, $P < 0.002$) and CVP ($r = 0.996$, $P < 0.0005$). These highly significant regression coefficients for correlation of the amount of Dys with systolic or diastolic performance support a tentative role for Dys in transmitting an effect through the actin–myosin linkage to the extracellular matrix. It is also noteworthy that no correlation was found between the amounts of Dys or the 60-kDa band and the dP/dt_{max} or dP/dt_{min} value (data not shown), both of which are regulated by Ca^{2+} handling (11) and the energetics of cardiac muscle cells (12). It should be emphasized that a distinct relationship was found between the amount of Dys or the 60-kDa band and the survival rate of the TO-2 animals over time (Fig. 2*b Lower*). It is possible that these immunological and hemodynamic data could be biased, because ≈30% of the TO-2 hamsters died of HF (Fig. 2*b Lower*), and we could only use the survivors in the analysis.

Effect of Long-Lasting Gene Therapy on Dys Localization. The final evidence that the disruption of Dys is not an epiphenomenon in HF but is actually caused by a loss of δ-SG is provided by the double immunostaining of Dys and δ-SG in TO-2 hearts with or without local gene transfection *in vivo* (Fig. 3*a*). In control F_1B hearts, both proteins were equally expressed on the SL (data not shown). In contrast, the TO-2 heart did not express δ-SG (13). As described above (Fig. 1), Dys staining became blurred with age, and some cardiomyocytes revealed Dys translocation (14). Gene delivery of normal δ-SG *in vivo*, by means of a nonpathogenic and long-lasting rAAV vector (7, 8), was used to locally express the δ-SG transgene, and this gene therapy completely ameliorated Dys translocation in the same cardiomyocytes for up to 35 weeks (Fig. 3*a Left*). In contrast, nontransfected cells

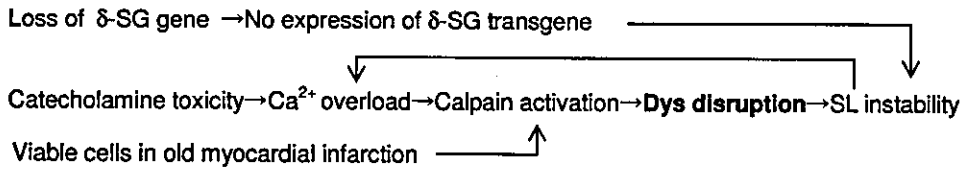

Scheme 1. Pathways for the progression of HF to an advanced stage.

showed translocation of Dys in the same sample (indicated by arrows in Fig. 3*a Right*). This finding specifically eliminates the possibility that Dys disruption resulted from the parallel development of HF, because Dys translocation was restricted to cardiomyocytes that did not express the δ-SG transgene. Furthermore, the amount of Dys estimated *in situ* by densitometry of immunofluoromicroscopic images in cardiomyocytes indicated a 1.22 ± 0.13 fold ($P < 0.01$) preferential localization of Dys on the SL of δ-SG-transfected cells ($n = 70$ cells per group).

Effect of Isp on SL Permeability, and Shift and Cleavage of Dys and δ-SG. A toxic dose of Isp (10 mg/kg i.p.) causes acute HF and morphological deterioration in normal rats (9). Pathological examination has shown time-dependent degradation of Dys and apoptosis of cardiomyocytes from 4 to 18 h after Isp was administered (15). Confocal microscopy of cardiomyocytes in the same observation field showed translocation of Dys (indicated by arrows in Fig. 3*b Left*) and entry of the SL-impermeable EB into the myoplasm of cardiac muscle cells. The shift of Dys was selectively detected 16 h after Isp treatment only in cardiomyocytes where EB had entered the myoplasm (Fig. 3*b Right*). Western blotting revealed time-dependent cleavage of Dys, showing degradation fragments between 60 and 200 kDa (Fig. 3*c Left*). In contrast, δ-SG was not hydrolyzed at all (Fig. 3*c Right*). Immunohistology confirmed that δ-SG did not shift from the SL but remained localized on the SL (data not shown). The effect of high-dose Isp, a β-adrenergic agonist, was similar to that observed in a DCM mouse with a protein kinase A knock-in gene (16). To verify the therapeutic effect of gene therapy in a β-adrenergic agonist/protein kinase A/phospholamban system, the pharmacological action (17, 18) and the disease prognosis need to be precisely examined, because an improvement in hemodynamics does not always prolong the lifespan of the animal (19).

The limited hydrolysis of Dys, common to the models of acute and chronic diseases in the present study, suggests a role for calpain, because cardiomyocytes contain an appreciable amount of this protein (20), and intracellular Ca^{2+} handling is modified in failing hearts (21, 22). Neither a specific inhibitor for calpain nor a calpain knockout animal is currently available to test this hypothesis. β-Adrenergic agonists induce Ca^{2+} overload in cardiomyocytes by increasing Ca^{2+} uptake (23). In addition, Dys and α-, β-, and γ-SG, but not δ-SG, are hydrolyzed by the endogenous protease (24) or isolated calpain *in vitro* (25, 26). The preferential breakdown of these proteins, but not δ-SG, in three HF models, i.e., TO-2 hamster hearts (13), Isp-treated rat hearts (Fig. 3*b*), and viable cells at the end stage of myocardial infarction (26), might be accompanied by substantially enhanced activity of *m*-calpain over its endogenous inhibitor, calpastatin. The expression of *m*-calpain in TO-2 hearts markedly exceeded that of calpastatin during the progression of HF (data not shown). These results may imply that the balance between calpain and calpastatin will shift in a calpain-dominant manner. Furthermore, dot hybridization analyses revealed no increment of mRNA of each DAP component under these HF conditions, suggesting that compensatory biosynthesis did not occur in the case of DAP.

A Scheme for the Progression of HF to an Advanced Stage. The clinical link between excess stimulation with catecholamines and myocardial damage has been confirmed by the therapeutic success of β-adrenergic antagonists in TO-2 hamsters (27) and humans (28, 29). The cleavage of Dys has also been documented after enterovirus infection, resulting in DCM-like HF (30). These pathological findings present a paradigm in which cardioselective cleavage of Dys may lead to progression of HF to an advanced stage (Scheme 1). Scheme 1 does not exclude the involvement of a protease cascade, as seen through the activation of a calpain-like homologue in neuronal degeneration in *Caenorhabditis elegans* (31), or involvement of the ubiquitin/proteasome system (32) in the loss of Dys. More definite evidence is required to precisely determine the causative factor(s). This common pathological process, irrespective of the hereditary or acquired origin and the chronic or acute course of the disease, suggests a strategy for the treatment of advanced HF through interruption of the vicious circle by either gene therapy or drug treatment.

We thank Dr. John R. Solaro (Department of Physiology and Biophysics, University of Illinois, Chicago) for discussion of the results and Dr. Y. Niwa and K. Kurosawa (Department of Pathophysiology, University of Tokyo) for experimental and secretarial assistance. This work was supported by Ministry of Education, Culture, and Science Grant A2 142070333 and by the Ministry of Welfare and Labor, Japan, the Mitsubishi Research Foundation, and the Motor Vehicle Foundation.

1. Cox, G. F. & Kunkel, L. M. (1997) *Curr. Opin. Cardiol.* **12**, 329–343.
2. Seidman, J. G. & Seidman, C. (2001) *Cell* **104**, 557–567.
3. Durbeej, M. & Campbell, K. P. (2002) *Curr. Opin. Genet. Dev.* **12**, 349–361.
4. Sakamoto, A., Ono, K., Abe, M., Jasmin, G., Eki, T., Murakami, Y., Masaki, T., Toyo-oka, T. & Hanaoka, F. (1997) *Proc. Natl. Acad. Sci. USA* **94**, 13873–13878.
5. Nigro, V., Okazaki, Y., Belsito, A., Piluso, G., Matsuda, Y., Politano, L., Nigro, G., Ventura, C., Abbondanza, C., Molinari, A. M., *et al.* (1997) *Hum. Mol. Genet.* **6**, 601–607.
6. Tsubata, S., Bowles, K. R., Vatta, M., Zintz, C., Titus, J., Muhonen, L., Bowles, N. E. & Towbin, J. A. (2000) *J. Clin. Invest.* **106**, 655–662.
7. Kawada, T., Sakamoto, A., Nakazawa, M., Urabe, M., Masuda, F., Hemmi, C., Wang, Y., Shin, W. S., Nakatsuru, Y., Sato, H., *et al.* (2001) *Biochem. Biophys. Res. Commun.* **284**, 431–435.
8. Kawada, T., Nakazawa, M., Nakauchi, S., Yamazaki, K., Shimamoto, R., Urabe, M., Nakata, J., Masui, F., Nakajima, T., Suzuki, J., *et al.* (2002) *Proc. Natl. Acad. Sci. USA* **99**, 901–906.
9. Kahn, D. S., Rona, G. & Chappel, C. I. (1969) *Ann. N.Y. Acad. Sci.* **156**, 285–293.
10. Vatta, M., Stetson, S. J., Perez-Verdia, A., Entman, M. L., Noon, G. P., Torre-Amione, G., Bowles, N. E. & Towbin, J. A. (2002) *Lancet* **359**, 936–941.
11. Ebashi, S., Nonomura, Y., Toyo-oka, T. & Katayama, E. (1976) *Symp. Soc. Exp. Biol.* **30**, 349–360.
12. Toyo-oka, T., Nagayama, K., Suzuki, J. & Sugimoto, T. (1992) *Circulation* **86**, 295–301.
13. Kawada, T., Nakatsuru, Y., Sakamoto, A., Koizumi, T., Shin, W. S., Okai-Matsuo, Y., Suzuki, J., Uehara, Y., Nakazawa, M., Satoh, H., *et al.* (1999) *FEBS Lett.* **458**, 405–408.
14. Kawada, T., Hemmi, C., Fukuda, S., Iwasawa, K., Tezuka, A., Nakazawa, M., Sato, H. & Toyo-oka, T. (2004) *Exp. Clin. Cardiol.* **8**, in press.
15. Xi, H., Shin, W. S., Suzuki, J., Nakajima, T., Kawada, T., Uehara, Y., Nakazawa, M. & Toyo-oka, T. (2000) *J. Cardiovasc. Pharmacol.* **36**, Suppl. 2, S25–S29.
16. Antos, C. L., Frey, N., Marx, S. O., Reiken, S., Gaburjakova, M., Richardson, J. A., Marks, A. R. & Olson, E. N. (2001) *Circ. Res.* **89**, 997–1004.

THE JOURNAL OF GENE MEDICINE
J Gene Med 2004; 6: 22–31.
Published online 5 November 2003 in Wiley InterScience (www.interscience.wiley.com). DOI: 10.1002/jgm.467

RESEARCH ARTICLE

In vivo expansion of gene-modified hematopoietic cells by a novel selective amplifier gene utilizing the erythropoietin receptor as a molecular switch

Takeyuki Nagashima[1]
Yasuji Ueda[1]*
Yutaka Hanazono[2]
Akihiro Kume[3]
Hiroaki Shibata[4]
Naohide Ageyama[4]
Keiji Terao[4]
Keiya Ozawa[3]
Mamoru Hasegawa[1]

[1]*DNAVEC Research Inc., Ibaraki 305-0856, Japan*

[2]*Division of Regenerative Medicine, Center for Molecular Medicine, Jichi Medical School, Tochigi 329-0498, Japan*

[3]*Division of Genetic Therapeutics, Center for Molecular Medicine, Jichi Medical School, Tochigi 329-0498, Japan*

[4]*Tsukuba Primate Center, National Institute of Infectious Diseases, Ibaraki 305-0843, Japan*

*Correspondence to: Yasuji Ueda, DNAVEC Research Inc., Ibaraki 305-0856, Japan.
E-mail: yueda@dnavec.co.jp

Received: 22 April 2003
Revised: 21 July 2003
Accepted: 21 July 2003

Abstract

Background *In vivo* expansion of gene-modified cells would be a promising approach in the field of hematopoietic stem cell gene therapy. To this end, we previously developed a selective amplifier gene (SAG), a chimeric gene encoding the granulocyte colony-stimulating factor (G-CSF) receptor (GCR), as a growth-signal generator and the hormone-binding domain of the steroid receptor as a molecular switch. We have already reported that hematopoietic cells retrovirally transduced with the SAG can be expanded in a steroid-dependent manner *in vitro* and *in vivo* in mice and nonhuman primates. In this study, we have developed a new-generation SAG, in which the erythropoietin (EPO) receptor (EPOR) is utilized instead of the steroid receptor as a molecular switch.

Methods Two EPO-driven SAGs were constructed, EPORGCR and EPORMpl, containing the GCR and c-Mpl as a signal generator, respectively. First, to compare the steroid-driven and EPO-driven SAGs, Ba/F3 cells were transduced with these SAGs. Next, to examine whether GCR or c-Mpl is the more suitable signal generator of the EPO-driven SAG, human cord blood $CD34^+$ cells were transduced with the two EPO-driven SAGs (EPORMpl and EPORGCR). Finally, we examined the *in vivo* efficacy of EPORMpl in mice. Irradiated mice were transplanted with EPORMpl-transduced bone marrow cells followed by administration of EPO.

Results The EPO-driven SAGs were shown to induce more rapid and potent proliferation of Ba/F3 cells than the steroid-driven SAGs. The EPORMpl induced more efficient EPO-dependent proliferation of the human cord blood $CD34^+$ cells than the EPORGCR in terms of total $CD34^+$ cell, c-Kit^+ cell, and clonogenic progenitor cell (CFU-C) numbers. In the transplanted mice the transduced peripheral blood cells significantly increased in response to EPO.

Conclusions The new-generation SAGs, especially EPORMpl, are able to efficiently confer an EPO-dependent growth advantage on transduced hematopoietic cells *in vitro* and *in vivo* in mice.

Keywords hematopoietic stem cells; gene therapy; $CD34^+$ cells; selective amplifier gene; *in vivo* expansion; retroviral vector

Introduction

One of the major obstacles associated with hematopoietic stem cell (HSC) gene therapy is the low efficiency of gene transfer into human HSCs with retroviral vectors [1]. The ability to positively select cells containing potentially therapeutic genes *in vivo* would represent an important tool for the clinical application of HSC gene therapy. A promising strategy of *in vivo* positive selection of transduced cells is to confer a direct proliferation advantage on gene-modified cells relative to their untransduced counterparts. We developed a chimeric gene designated 'selective amplifier gene' (SAG) which encodes a chimeric receptor between the granulocyte colony-stimulating factor (G-CSF) receptor (GCR) and the hormone-binding domain of the estrogen or tamoxifen receptor. The GCR moiety is a growth-signal generator and the estrogen receptor (ER) moiety is a molecular switch to regulate (turn on or off) the growth signal generated from the GCR. We previously showed that hematopoietic cells transduced with the SAG can be selectively expanded in an estrogen- or tamoxifen-dependent manner *in vitro* [2–5] and *in vivo* in mice and nonhuman primates [6,7]. In nonhuman primates, however, some animals that received the SAG did not show an increase in transduced cells in response to estrogen or tamoxifen, suggesting that the SAG was not potent enough to achieve *in vivo* expansion in all animals [7].

The utilization of the steroid receptor as a molecular switch may have attenuated the potency of the SAG. The estrogen-mediated dimerization of the chimeric molecule may be less efficient than the natural ligand (G-CSF)-mediated dimerization. In fact, the fusion protein between the GCR and estrogen receptor responds to G-CSF more efficiently than to estrogen [2]. To rectify this problem, we utilized the erythropoietin receptor (EPOR) instead of the steroid receptor as a molecular switch. Since the EPOR is a member of the cytokine receptor superfamily [8], the fusion proteins between the EPOR and other cytokine receptors such as the GCR should be more stable and compatible than the prototype fusion protein. In addition, the EPOR is not expressed on immature hematopoietic cells and thus can be used as a selective switch for these cells [9]. Of note, recombinant human erythropoietin (EPO) has already been used widely in clinical application and can be administered repeatedly to human subjects without serious adverse effects [10,11].

On the other hand, as a growth-signal generator, we tried to use the thrombopoietin (TPO) receptor, c-Mpl, in addition to the GCR. It has been reported that c-Mpl is expressed on very immature hematopoietic cells and that TPO actually stimulates the growth of these cells [12–15]. In fact, the cytoplasmic fragment of c-Mpl has already been used for the purpose of cell expansion [5,16]. The intracellular signal from c-Mpl may thus be more appropriate than that from the GCR for expansion of hematopoietic stem/progenitor cells. In the present study, we examined the efficacy of these new generation SAGs *in vitro* and *in vivo* in mice.

Materials and methods

Cell lines

Ba/F3 cells were maintained in Dulbecco's modified Eagle's medium (DMEM; Gibco-BRL, Grand Island, NY, USA) supplemented with 10% fetal bovine serum (FBS; Gibco-BRL), 1% penicillin/streptomycin (Gibco-BRL), and 1 ng/ml recombinant mouse IL-3 (rmIL-3; Gibco-BRL). The ecotropic packaging cell line BOSC23 [17] and human embryonic kidney 293T cells were maintained in DMEM containing 10% FBS and 1% penicillin/streptomycin.

Plasmid construction

The wild-type human erythropoietin receptor (EPORwt) cDNA was obtained from pCEP4-EPOR (kindly provided by Dr. R. Kralovics, University of Alabama, USA) [18]. The fragment containing the murine phosphoglycerate kinase (pgk) promoter and neomycin phosphotransferase gene (neo) (EcoRI-BamHI) in the retroviral plasmid pMSCV2.2 (kindly provided by Dr. R. G. Hawley, University of Toronto, Canada) [19] was replaced by the EPORwt cDNA (EcoRI-BamHI) to construct pMSCV-EPORwt.

pMSCV-EPORGCR and pMSCV-EPORMpl were constructed as follows. The cytoplasmic region of murine G-CSF receptor (GCR) cDNA was obtained by PCR using pMSCV-ΔY703FGCRER as a template [3] with the primer pair 5′-AAG GAT CCA AAC GCA GAG GAA AGA AGA CT-3′ and 5′-AAG TCG ACC TAG AAA CCC CCT TGT TC-3′. The cDNA coding to the cytoplasmic region of human TPO receptor (c-Mpl) was obtained by PCR using pcDNA3.1-c-Mpl (provided by Dr. M. Takatoku, Jichi Medical School, Tochigi, Japan) [20] as a template with the primer pair 5′-AAG GAT CCA GGT GGC AGT TTC CTG CA-3′ and 5′-CGG TCG ACT CAA GGC TGC TGC CAA TA-3′. The fragment containing the extracellular plus transmembrane region of the human EPOR cDNA was obtained by PCR using pCEP4-EPOR as a template with the primer pair 5′-CTC GGC CGG CAA CGG CGC AGG GA-3′ and 5′-AAG GAT CCC AGC AGC GCG AGC ACG GT-3′. The fragment containing the extracellular plus transmembrane region of human EPOR cDNA and the fragment containing the cytoplasmic region of murine GCR or human c-Mpl were cloned into the EcoRI-SalI site of pBluescript SK (pSK; Stratagene, La Jolla, CA, USA) to construct pSK-EPOGCR or pSK-EPOMpl, respectively. The pgk promoter/neo cassette (EcoR-SalI) in pMSCV was replaced by the EcoRI-SalI fragment containing the EPORGCR or EPORMpl cDNA each from pSK-EPORGCR or pSK-EPORMpl, respectively. The resultant construct was designated as pMSCV-EPORGCR or pMSCV-EPORMpl, respectively.

pMSCV-EPORwt-ires-mitoEYFP, pMSCV-EPORGCR-ires-mitoEYFP, and pMSCV-EPORMpl-ires-mitoEYFP were

constructed as follows. The internal ribosome entry site (ires) sequence derived from pIRES-EGFP (Clontech, Palo Alto, CA, USA) and the mitoEYFP cDNA derived from pEYFP-Mito (Clontech) were inserted into the PstI-BamHI site and the SpeI-NotI site of pSK, respectively. The resultant plasmid was pSK-ires-mitoEYFP. The mitEYFP cDNA encodes the enhanced yellow fluorescent protein (enhanced YFP, EYFP) linked to a mitochondria localization signal sequence so that EYFP is sequestered inside the mitochondria, thus circumventing the presumed toxicity of YFP [21]. The blunted fragment encoding the ires-mitoEYFP cDNA was ligated into the ClaI blunted site of pMSCV-EPORwt, pMSCV-EPORGCR, and pMSCV-EPORMpl to obtain pMSCV-EPORwt-ires-mitoEYFP, pMSCV-EPORGCR-ires-mitoEYFP, and pMSCV-EPORMpl-ires-mitoEYFP, respectively. The final plasmids were certified as correct by sequence analysis.

Retroviral vectors

To obtain ecotropic retroviral vectors, BOSC23 cells were transfected with mouse stem cell virus (MSCV)-based retroviral plasmids (derivatives from pMSCV, see above) using Lipofectamine Plus (Invitrogen, San Diego, CA, USA) according to the manufacturer's protocol and the supernatants containing the ecotropic retroviral vectors were harvested 48–72 h post-transfection. The titers were 1×10^6/ml as assessed by RNA dot-blot. To obtain amphotropic retroviral vectors, 293T cells were transfected with MSCV-based retroviral plasmids along with pCL-Ampho (Imgemex, San Diego, CA, USA) using Lipofectamine Plus and the supernatants containing the amphotropic retroviral vectors were harvested 48–72 h post-transfection. The titers were 1×10^6/ml as assessed by RNA dot-blot.

Retroviral transduction and culture

Ba/F3 cells were suspended in 1 ml retroviral supernatant containing 10 ng/ml rmIL-3 at a density of 1×10^5 cells/ml, and transferred to 12-well plates coated with 20 μg/cm^2 of RetroNectin (Takara Bio, Shiga, Japan) [22]. The cells were incubated at 37 °C in a humidified atmosphere of 5% CO_2 in air for 24 h. During this period, culture medium was replaced by fresh viral supernatant twice (every 12 h). After retroviral infection, YFP-positive cells were isolated using an EPICS ELITE cell sorter (Coulter, Miami, FL, USA). The purity of sorted YFP-positive cells was greater than 98%. The sorted Ba/F3 cells were subjected to further liquid culture (described above) or cell proliferation assays (see below).

Human cord blood CD34$^+$ cells (BioWhittaker, Walkersville, MD, USA) were thawed and placed in 12-well plates coated with 20 μg/cm^2 of RetroNectin and cultured for 24 h at 37 °C with 5% CO_2 in Iscove's modified Dulbecco's medium (IMDM; Gibco-BRL) supplemented with 10% FBS (Hyclone, Logan, UT, USA), 50 ng/ml recombinant human interleukin 6 (rhIL-6; Ajinomoto, Osaka, Japan), 100 ng/ml recombinant human stem cell factor (rhSCF; Biosource, Camarillo, CA, USA), 100 ng/ml recombinant human Flt-3 ligand (Research Diagnostic, Flanders, NJ, USA), and 100 ng/ml recombinant human thrombopoietin (rhTPO; Kirin, Tokyo, Japan). The cells were then resuspended in 1 ml viral supernatant containing the same cytokines as described above at a starting density of 1×10^5 cells/ml. During the transduction period (48 h), culture medium was replaced by fresh viral supernatant four times (every 12 h). After retroviral transduction, human cord blood CD34$^+$ cells were washed twice and cultured in IMDM medium containing 10% FBS (Hyclone) and 1% penicillin/streptomycin in the presence of 10 ng/ml recombinant human EPO (rhEPO; Roche Diagnostics, Mannheim, Germany) in a 37 °C 5% CO_2 incubator. The cells were subjected to flow cytometry or colony assay (see below) on indicated days.

Cell proliferation assay

Ba/F3 proliferation assay was performed using the CellTier 96 Aqueous One Solution cell proliferation assay (Promega, Madison, WI, USA) according to the manufacturer's instructions. In brief, 20 μl MTS (3-[4,5-dimethylthiazol-2-yl]-5-[3-carboxymethoxyphenyl]-2-[4-sulfophenyl]-2*H*-tetrazolium)-labeling mixture was added to each well of 96-well dishes containing cells to be assayed. Following incubation at 37 °C for 2 h, the spectrophotometric absorbance was measured at wavelengths of 490 and 650 nm. A_{490}-A_{650} values were used to determine Ba/F3 cell proliferation. Experiments were conducted in triplicate.

Flow cytometry

Human cord blood CD34$^+$ cells were washed and resuspended in CellWASH (Becton Dickinson, San Jose, CA, USA). The cells were then incubated with phycoerythrin (PE)-labeled anti-c-Kit (Nichirei, Tokyo, Japan), PE-labeled anti-glycophorin A (Nichirei), PE-labeled anti-CD41 (Nichirei), or PE-labeled anti-CD15 (Immunotech, Marseille, France) at 4 °C for 30 min. The cells were washed once and subjected to a FACSCalibur (Becton Dickinson) using excitation at 488 nm. Untransduced cells served as negative controls.

For mouse blood samples, blood cells were suspended in ACK lysis buffer (155 mM NH_4Cl, 10 mM $KHCO_3$, and 0.1 mM EDTA; Wako, Osaka, Japan) to dissolve red blood cells. The cells were washed once and subjected to a FACSCalibur (Becton Dickinson) using excitation at 488 nm.

Colony assay and PCR

Human cord blood CD34$^+$ cells were plated in 35-mm dishes with α-minimum essential medium (Gibco-BRL)

containing 1.2% methylcellulose (Shinetsu Kagaku, Tokyo, Japan) supplemented with 20% FBS (Intergen, Purchase, NY, USA) and 1% bovine serum albumin (Sigma, St. Louis, MO, USA) in the presence of 100 ng/ml rhSCF, 100 ng/ml rhIL-6, and 100 ng/ml recombinant human interleukin 3 (rhIL-3; PeproTech, London, UK), or in the presence of 20 ng/ml of rhEPO alone. After incubation for 14 days at 37 °C in a humidified atmosphere of 5% CO_2 in air, colonies were scored under an inverted microscope. The experiments were performed in triplicate.

Colonies in methylcellulose culture were plucked up under an inverted microscope, suspended in 50 µl of distilled water, and digested with 20 µg/ml proteinase K (Takara) at 55 °C for 1 h followed by incubation at 99 °C for 10 min. PCR was performed to amplify the 351-bp sequence using the EYFP sense primer (5′-CGT CCA GGA GCG CAC CAT CTT C-3′) and antisense primer (5′-AGT CCG CCC TGA GCA AAG ACC-3′). To certify the initial DNA amounts, the β-actin genomic DNA fragment was simultaneously amplified using the sense primer (5′-CAT TGT CAT GGA CTC TGG CGA CGG-3′) and antisense primer (5′-CAT CTC CTG CTC GAA GTC TAG GGC-3′). Amplification conditions were 95 °C for 1min, 55 °C for 30 s, and 72 °C for 30 s with 35 cycles.

Mouse transplantation

Eight-week-old C57Bl/6 mice (Charles River Japan, Yokohama, Japan) intraperitoneally received 150 µg/kg 5-fluorouracil (Sigma). Forty-eight hours after injection, bone marrow cells were harvested from the femora of each mouse. Cells were cultured in IMDM (Gibco-BRL) containing 20% FBS (Hyclone) and 20 ng/ml rhIL-6 and 100 ng/ml recombinant rat SCF (provided by Amgen) for 48 h. The cells were then placed in 6-well plates coated with 20 µg/cm^2 of RetroNectin and resuspended in IMDM supplemented with 10% FBS (Hyclone) and the aforementioned cytokines at a starting density of 5×10^5 cells/ml. During the transduction period (48 h), culture medium was replaced by fresh viral supernatant four times (every 12 h). The cells were harvested after a total of 96 h (4 days) in culture, washed with PBS three times, and injected into 8-week-old female C57/Bl6 mice that had been irradiated with 800 cGy. After transplantation, some mice received recombinant mouse EPO (rmEPO; 200 IU/kg, Roche Diagnostics) in a total volume of 100 µl via the tail vein three times a week. To avoid development of anemia after drawing blood from the transplanted mice, blood was transfused into the mice via the tail vein at the time of blood drawing. The blood for transfusion was drawn from donor C57/Bl6 mice and pooled. It was irradiated with 20 Gy and diluted with physiological salt solution prior to transfusion. Peripheral blood mononuclear cells of the recipient mice were analyzed for EYFP expression by flow cytometry.

Results

A new generation SAG

The structure of the SAGs is shown in Figure 1. The prototype SAG (steroid-driven SAG) is a chimeric gene encoding the G-CSF receptor (GCR) and the estrogen receptor hormone-binding domain. In the GCR, the ligand (G-CSF)-binding domain was deleted to remove the responsiveness to endogenous G-CSF [2]. The tyrosine residue at the 703rd amino acid in the GCR was replaced by phenylalanine to hamper the differentiation signal [3]. In addition, another mutation (G525R) was introduced into the estrogen receptor hormone-binding domain to evade the responsiveness to endogenous estrogen without impairing the responsiveness to synthetic hormones such as tamoxifen [4]. In this study, we constructed a new generation SAG, in which the erythropoietin (EPO) receptor (EPOR) is utilized instead of the estrogen or tamoxifen receptor as a molecular switch. Two types of EPO-driven SAG were constructed, EPORGCR and EPORMpl, containing the GCR gene and the thrombopoietin (TPO)

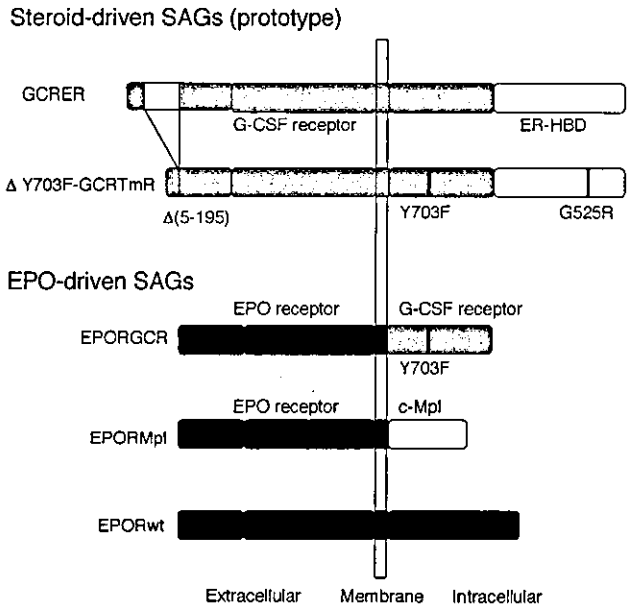

Figure 1. The structure of SAGs. The GCRER is a prototype of the selective amplifier gene (SAG), a chimeric gene encoding the G-CSF receptor (GCR) as a growth-signal generator and the estrogen receptor hormone-binding domain (ER-HBD) as a molecular switch. In ΔY703F-GCRTmR, the G-CSF-binding domain was deleted from the GCR gene to abolish responsiveness to endogenous G-CSF, a point mutation (Y703F) was introduced into the GCR moiety to disrupt the differentiation signal generated by the GCR, and another point mutation (G525R) was introduced into the ER-HBD moiety to evade responsiveness to endogenous estrogen without impairing responsiveness to a synthetic hormone tamoxifen. In the new SAG, the erythropoietin (EPO) receptor (EPOR) was utilized instead of the estrogen or tamoxifen receptor as a molecular switch. To construct it, the intracellular domain of the wild-type EPOR (EPORwt) gene was replaced by that of the GCR or thrombopoietin receptor (c-Mpl) gene as a growth-signal generator